AIMS Mathematics, 9(6): 15671–15698.
DOI: 10.3934/math.2024756
Received: 03 March 2024
Revised: 02 April 2024
Accepted: 09 April 2024
Published: 30 April 2024

http://www.aimspress.com/journal/Math

Research article

Piecewise approximate analytical solutions of high-order reaction-diffusion singular perturbation problems with boundary and interior layers

Essam R. El-Zahar[1,2,*], Ghaliah F. Al-Boqami[1] and Haifa S. Al-Juaydi[1]

[1] Department of Mathematics, College of Science and Humanities in Al-Kharj, Prince Sattam bin Abdulaziz University, Al-Kharj 11942, Saudi Arabia; Galiahfr@gmail.com, hs.aljuaydi@psau.edu.sa
[2] Department of Basic Engineering Sciences, Faculty of Engineering, Menoufia University, Shebin El-Kom 32511, Egypt

* **Correspondence:** Email: er.elzahar@psau.edu.sa.

Abstract: This work aims to present a reliable algorithm that can effectively generate accurate piecewise approximate analytical solutions for third- and fourth-order reaction-diffusion singular perturbation problems. These problems involve a discontinuous source term and exhibit both interior and boundary layers. The original problem was transformed into a system of coupled differential equations that are weakly interconnected. A zero-order asymptotic approximate solution was then provided, with known asymptotic analytical solutions for the boundary and interior layers, while the outer region solution was obtained analytically using an enhanced residual power series approach. This approach combined the standard residual power series method with the Padé approximation to yield a piecewise approximate analytical solution. It satisfies the continuity and smoothness conditions and offers higher accuracy than the standard residual power series method and other numerical methods like finite difference, finite element, hybrid difference scheme, and Schwarz method. The algorithm also provides error estimates, and numerical examples are included to demonstrate the high accuracy, low computational cost, and effectiveness of the method within a new asymptotic semi-analytical numerical framewor.

Keywords: singular perturbation theory; boundary value problems; discontinuous source term asymptotic approximation; residual power series method; Padé approximant

Mathematics Subject Classification: 34B08, 34D15, 35A22, 44A10

Abbreviations

Abbreviations	Name
SPPs	Singular perturbation problems
SPBVPs	Singular perturbation boundary value problems
IVPs	Initial value problems
RPSM	Residual power series method
RPSPM	Residual power series method in conjunction with Pade approximants
ε	Perturbation parameter
$\vec{y}_{as}$	Asymptotic expansion for the solution of the third-order SPBVP
$\vec{u}$	The reduced problem solution for third-order SPBVPs
$\vec{v}_L, \vec{v}_R$	The left layer corrections of the third-order SPBVP
$\vec{w}_L, \vec{w}_R$	The right layer corrections of the third-order SPBVP
$\vec{\hat{y}}_{as}$	Asymptotic expansion for the solution of the fourth-order SPBVP
$\vec{\hat{u}}$	The reduced problem solution for fourth-order SPBVPs
$\vec{\hat{v}}_L, \vec{\hat{v}}_R$	The left layer corrections of the fourth-order SPBVP
$\vec{\hat{w}}_L, \vec{\hat{w}}_R$	The right layer corrections of the fourth-order SPBVP
$Res^{\infty}(x)$	The ∞^{th}-residual function
$Res^{k}(x)$	The k^{th}-residual function
r_m	Power series coefficient
$p_l(x)$	Polynomial of degree l
$q_n(x)$	Polynomial of degree n
$\vec{u}^{[l,n]}$	Padé approximant of the truncated series solution $u^k(x)$
$\vec{\hat{u}}^{[l,n]}$	Padé approximant of the truncated series solution $\hat{u}^k(x)$
$\vec{y}_{ap}$	The piecewise approximate analytical solution of the third-order SPBVP
$\vec{\hat{y}}_{ap}$	The piecewise approximate analytical solution of the fourth-order SPBVP

1. Introduction

Singular perturbation problems (SPPs) manifest in various domains of applied mathematics and engineering, including control theory [1], fluid flow at high Reynolds or Hartmann numbers [2,3], heat and mass transfer [4], chemical reaction in spark ignition turbocharger engine [5], wave dynamics in coastal and ocean engineering [6], semiconductor devices, nuclear physics, etc. [7,8]. These problems are distinguished by their solutions that display a multiscale behavior, featuring boundary/interior layers where the solution experiences rapid fluctuations. In contrast, outside of these layers, the solution transitions smoothly and gradually. In SPPs, the perturbation parameter represents a small ratio of physical quantities that varies across applications. For instance, in fluid mechanics, it may represent the ratio of suction/injection velocities to flow velocity, the inverse of a high Prandtl number, or the ratio of the viscous forces to the inertial forces. In heat transfer, it represents the ratio of thermal conductivity to heat capacity. In chemical reactions, it represents the ratio of diffusion to reaction. In satellite orbits, it represents drag coefficients. In planetary rings, it represents the inverse of a large azimuthal number. In reaction-diffusion problems, it represents the ratio of diffusion coefficient to reaction rate [7,8]. To handle and solve SPPs, a range of numerical and analytical approaches have been developed and investigated in studies conducted by O'Malley [7], Miller et al. [9], Liu et al. [10], and other referenced works. Traditional numerical methods often provide accurate approximate solutions for SPPs, particularly in the presence of very thin layer regions. This is due to the high

stiffness and multiscale solution gradients that are characteristic of these regions [9,10]. To tackle this obstacle, certain numerical techniques employ a strategy of converting second-order singular perturbation boundary value problems (SPBVPs) into initial value problems (IVPs). This approach is preferred because the numerical treatment of the corresponding IVPs is generally regarded as more straightforward than that of BVPs. Various initial value techniques have been developed and discussed for solving SBVPs. These techniques address second-order problems [2,11], higher-order problems [12,13], and systems of equations [14,15]. While extensive research has been conducted on SPBVPs, most computational studies have focused on second-order problems. Higher-order SPBVPs have received less attention, with most works focusing on problems with smooth data. These studies have primarily addressed third-order [16–18], fourth-order [12,19], and fifth-order problems [20].

However, some authors have specifically addressed problems with discontinuous data. Notably, prominent approaches for tackling third- and fourth-order SPBVPs with a discontinuous source term include the nonuniform mesh finite difference method [21,22], fitted mesh finite element method [23,24], hybrid difference scheme [25], Schwarz method [26], and Haar wavelets [27]. However, most methods developed for high-order SPBVPs are numerical in nature, highlighting the need for alternative methods that can provide accurate approximate analytical solutions. Obtaining accurate analytical solutions for these SPBVPs is crucial, as it enables researchers to meticulously examine how various physical parameters influence the behavior of the solutions. Among different methods devised to obtain analytical approximations for the solutions of differential equations, we can use the homotopy perturbation method [28,29], differential transform method [30–32], and residual power series method (RPSM) [33–35], among others. The RPSM is a robust technique for solving IVPs without requiring linearization, perturbation, or discretization. It offers an alternative to computationally intensive classical power series methods. However, the RPSM and other Taylor series approximation methods have limitations, particularly when applied to problems with non-smooth solutions, large time spans, singularities, or high solution gradients, such as those involving boundary layers [30,36,37]. To overcome these challenges, an enhanced version of the RPSM is proposed, which incorporates Padé approximants known for their superior convergence compared to series approximations [31,37].

This work presents a reliable algorithm for constructing piecewise approximate analytical solutions for third- and fourth-order reaction-diffusion SPBVPs with a discontinuous source term. The algorithm transforms the original problem into a set of weakly coupled differential equations and provides a zero-order asymptotic approximate solution with known asymptotic analytical solutions for the boundary and interior layers. The outer region solution is obtained analytically by solving the reduced problem, which is independent of the perturbation parameter, using an enhanced residual power series approach that combines the standard RPSM with the Padé approximation (RPSPM). This approach results in a piecewise approximate analytical solution that satisfies continuity and smoothness conditions. By combining the outer region solution with the known analytical solutions for the boundary and interior layers, the piecewise approximate analytical solution for the original SPBVP is obtained. The method's accuracy is assessed through error estimation. The present method is more accurate than the standard RPSM and other numerical asymptotic methods like the finite difference [22], the finite element [23], the hybrid difference scheme [25], and the Schwarz method [26]. The algorithm also provides error estimates, and numerical examples are included to demonstrate the high accuracy, low computational cost, and effectiveness of the method within a new asymptotic semi-analytical numerical framework.

2. Description of the method

Consider the following two reaction-diffusion SPBVPs:

(a) **Third-order SPBVP** [22,23,25]

$$\begin{cases} -\varepsilon y'''(x) + b(x)y'(x) + c(x)y(x) = f(x), x \in (\bar{\Omega}), \\ y(0) = p, y'(0) = q, y'(1) = r, \end{cases} \tag{1}$$

where y is a function that belongs to the set $C^1(\bar{\Omega}) \cap C^2(\Omega) \cap C^3(\bar{\Omega})$C, while $b(x)$ and $c(x)$ are regarded as adequately smooth over $\bar{\Omega}$ and fulfill the following imposed conditions:

$$\begin{aligned} &b(x) \geq \beta > 0, \\ &0 \geq c(x) \geq -\gamma, \gamma > 0, \\ &\beta - \theta\gamma \geq \eta > 0, \end{aligned}$$

for some η, and arbitrarily value of θ greater than and close to 2.

(b) **Fourth-order SPBVP** [21,26,27]

$$\begin{aligned} -\varepsilon\tilde{y}^{(iv)}(x) + b(x)\tilde{y}''(x) - \tilde{c}(x)\tilde{y}(x) = -f(x), x \in (\bar{\Omega}), \\ \tilde{y}(0) = p, \tilde{y}(1) = q, \tilde{y}''(0) = -r, \tilde{y}''(1) = -s, \end{aligned} \tag{2}$$

where $\tilde{y}$ is a function that belongs to the set $C^2(\bar{\Omega}) \cap C^3(\Omega) \cap C^4(\bar{\Omega})$, while $b(x)$ and $\tilde{c}(x)$ are regarded as adequately smooth over $\bar{\Omega}$ and fulfill the following imposed conditions:

$$\begin{aligned} &b(x) \geq \beta > 0, \\ &0 \geq \tilde{c}(x) \geq \gamma, \gamma > 0, \\ &\beta - \theta\gamma \geq \eta > 0, \end{aligned}$$

for some η, and arbitrarily value of θ greater than and close to 2.

For both problems defined above, $\Omega = (0,1), \Omega^- = (0,d), \Omega^+ = (d,1), \bar{\Omega} = \Omega^- \cup \Omega^+ = \Omega \setminus \{d\}$ and ε is a small positive parameter, $0 < \varepsilon < 1$. It is assumed that the function $f(x)$ has a jump discontinuity at the point d and sufficiently smooth in the rest of the domain $\Omega \setminus \{d\}$. This discontinuity leads to the appearance of an interior layer in the first derivative $y'(x)$ of the problem (1) and in the second derivative $\tilde{y}''(x)$ of the problem (2) [23,25]. These interior layers are a common feature in many physical systems due to changes in the sources, including fluid mechanics, heat transfer, and electromagnetics, and have important applications such as aircraft design, heat exchanger optimization, and electromagnetic device development [38–40]. In fluid mechanics, shock waves arise when a fluid undergoes a sudden change in velocity or pressure, such as in the case of a supersonic aircraft [38]. In heat transfer, interior layers appear in Stefan problems, which involve phase changes such as the melting of a solid or the boiling of a liquid [39]. In electromagnetics, interior layers can form in fields with conductors or dielectrics due to changes in the material properties [40].

The third-order SPBVP (1) can be converted into an equivalent problem that takes the following form [22,23]:

$$\begin{cases} y_1'(x) - y_2(x) = 0, x \in (0,1], \\ -\varepsilon y_2''(x) + b(x)y_2(x) + c(x)y_1(x) = f(x), x \in (\bar{\Omega}), \\ y_1(0) = p, y_2(0) = q, y_2(1) = r, \end{cases} \tag{3}$$

where

$$y_1(x) = y(x), y_2(x) = y'^{(x)}, \vec{y}(x) = \big(y_1(x), y_2(x)\big),$$

$$y_1(x) \in C^1(\bar{\Omega}) \cap C^2(\Omega) \cap C^3(\bar{\Omega}), y_2(x) \in C^0(\bar{\Omega}) \cap C^1(\Omega) \cap C^2(\bar{\Omega}).$$

Similarly, the fourth-order SPBVP (2) can be transformed into [21,23].

$$\begin{cases} \hat{y}_1''(x) + \hat{y}_2(x) = 0, x \in \Omega, \\ -\varepsilon \hat{y}_2''(x) + b(x)\hat{y}_2(x) + \tilde{c}(x)\hat{y}_1(x) = f(x), x \in (\bar{\Omega}), \\ \hat{y}_1(0) = p, \hat{y}_1(1) = q, \hat{y}_2(0) = r, \hat{y}_2(1) = s, \end{cases} \tag{4}$$

where

$$\hat{y}_1(x) = \tilde{y}(x), \hat{y}_2(x) = -\tilde{y}''^{(x)}, \vec{\hat{y}}(x) = \left(\hat{y}_1(x), \hat{y}_2(x)\right),$$

$$\hat{y}_1(x) \in C^2(\bar{\Omega}) \cap C^3(\Omega) \cap C^4(\bar{\Omega}), \hat{y}_2(x) \in C^0(\bar{\Omega}) \cap C^1(\Omega) \cap C^2(\bar{\Omega}).$$

Using some standard perturbation methods [7,11], an asymptotic expansion for the solution of (3) can be constructed as follows [22,23,25]:

$$\vec{y}_{as} = \vec{u} + \begin{cases} \vec{v}_L + \vec{w}_L, \ x \in \Omega^- \cup \{0, \mathrm{d}\}, \\ \vec{v}_R + \vec{w}_R, \ x \in \Omega^+ \cup \{1\}, \end{cases} \tag{5}$$

where

$$\vec{y}_{as} = \left(y_{1,as}(x), y_{2,as}(x)\right)^T, \vec{u} = \left(u_1(x), u_2(x)\right)^T, \vec{v}_L = (v_{1L}, v_{2L})^T,$$

$$\vec{w}_L = (w_{1L}, w_{2L})^T, \vec{v}_R = (v_{1R}, v_{2R})^T, \vec{w}_R = (w_{1R}, w_{2R})^T.$$

The functions $u_1(x), u_2(x)$ are continuous ones and satisfy the reduced problem of (3)

$$\begin{cases} u_1'(x) - u_2(x) = 0, x \in (0,1], \\ b(x)u_2(x) + c(x)u_1(x) = f(x), x \in \bar{\Omega}, \\ u_1(0) = p, \end{cases} \tag{6}$$

and

$$\vec{v}_L = (v_{1L}, v_{2L})^T, \vec{v}_R = (v_{1R}, v_{2R})^T$$

are the left layer corrections that defined by

$$v_{1L}' = v_{2L}, \qquad v_{2L} = k_1 e^{-x\sqrt{\frac{b(0)}{\varepsilon}}}, \qquad x \in \{0\} \cup \Omega^-,$$

$$v_{1R}' = v_{2R}, \qquad v_{2R} = k_2 e^{-(x-d)\sqrt{\frac{b(d)}{\varepsilon}}}, \qquad x \in \Omega^+ \cup \{1\},$$

while

$$\vec{w}_L = (w_{1L}, w_{2L})^T, \vec{w}_R = (w_{1R}, w_{2R})^T$$

are the right layer corrections and defined by

$$w_{1L}' = w_{2L}, \ w_{2L} = k_3 e^{-(d-x)\sqrt{\frac{b(d)}{\varepsilon}}}, \ x \in \{0\} \cup \Omega^-,$$

$$w_{1R}' = w_{2R}, \qquad w_{2R} = k_4 e^{-(1-x)\sqrt{\frac{b(1)}{\varepsilon}}}, \qquad x \in \Omega^+ \cup \{1\}.$$

The constants k_1, k_2, k_3 and k_4 are chosen such that $y_{2,as} \in C^0(\bar{\Omega}) \cap C^1(\Omega)$, that is,

$$y_{2,as}(0) = y_2(0), y_{2,as}(1) = y_2(1),$$
$$y_{2,as}(d^+) = y_{2,as}(d^-), y'_{2,as}(d^+) = y'_{2,as}(d^-).$$

The constants are given by [22,23]

$$k_1 = [y_2(0) - u_2(0)] - k_2 e^{-d\sqrt{\frac{b(d)}{\varepsilon}}},$$

$$k_2 = \left(\frac{k_{21}\left(\sqrt{b(d)}+\sqrt{p(1)}e^{-(1-d)\sqrt{\frac{b(d)+b(1)}{\varepsilon}}}\right)}{k_{24}+k_{25}} + \frac{(k_{22}+k_{23})(1-e^{\frac{-(1-d)\sqrt{(b(d)+b(1))}}{\varepsilon}})}{k_{24}+k_{25}}\right),$$

$$k_{21} = [(y_2(1) - u_2(1))e^{-(1-d)\sqrt{\frac{b(1)}{\varepsilon}}} - (y_2(0) - u_2(0))e^{-d\sqrt{\frac{b(0)}{\varepsilon}}}] + [u_2(d^+) - u_2(d^-)],$$

$$k_{22} = \sqrt{b(1)}\big(y_2(1) - u_2(1)\big)e^{-(1-d)\sqrt{\frac{b(1)}{\varepsilon}}} + \sqrt{b(0)}(y_2(0) - u_2(0))e^{-d\sqrt{\frac{b(0)}{\varepsilon}}},$$

$$k_{23} = \sqrt{\varepsilon}[u_2(d^+) - u_2(d^-)],$$

$$k_{24} = (\sqrt{b(d)} + \sqrt{b(1)}e^{-(1-d)\sqrt{\frac{b(1)+b(d)}{\varepsilon}}})(1 - e^{-d\sqrt{\frac{b(0)+b(d)}{\varepsilon}}}),$$

$$k_{25} = \left(\sqrt{b(d)} + \sqrt{b(0)}e^{-d\sqrt{\frac{b(0)+b(d)}{\varepsilon}}}\right)\left(1 - e^{-(1-d)\sqrt{\frac{b(1)+b(d)}{\varepsilon}}}\right),$$

$$k_3 = \frac{k_{31}+k_{32}}{k_{33}},$$

$$k_{31} = [y_2(0) - u_2(0)]e^{-d\sqrt{\frac{b(0)}{\varepsilon}}} + k_2(1 - e^{-d\sqrt{\frac{b(0)+b(d)}{\varepsilon}}}),$$

$$k_{32} = [u_2(d^+) - u_2(d^-)] - [y_2(1) - u_2(1)]e^{-(1-d)\sqrt{\frac{b(1)}{\varepsilon}}},$$

$$k_{33} = (1 - e^{-(1-d)\sqrt{\frac{b(d)+b(1)}{\varepsilon}}}),$$

$$k_4 = [y_2(1) - u_2(1)] - k_2 e^{-(1-d)\sqrt{\frac{b(d)}{\varepsilon}}}.$$

Theorem 2.1. [22,23,25] The asymptotic expansion of zero-order, denoted as $\vec{y}_{as}(x)$ as defined previously in (5) and (6) for the solution $\vec{y}(x)$ of the SBVP (3) satisfies the inequality

$$\| \vec{y}(x) - \vec{y}_{as}(x) \|_\infty \leq C\sqrt{\varepsilon}, x \in \bar{\Omega}. \tag{7}$$

Similarly, an asymptotic expansion for the solution of (4) can be constructed as follows [21,23,25]:

$$\vec{\hat{y}}_{as} = \vec{\hat{u}} + \begin{cases} \vec{\hat{v}}_L + \vec{\hat{w}}_L, & x \in \Omega^- \cup \{0, \mathrm{d}\}, \\ \vec{\hat{v}}_R + \vec{\hat{w}}_R, & x \in \Omega^+ \cup \{1\}, \end{cases} \tag{8}$$

where

$$\vec{\hat{y}}_{as} = \left(\hat{y}_{1,as}(x), \hat{y}_{2,as}(x)\right)^T, \vec{\hat{u}} = \left(\hat{u}_1(x), \hat{u}_2(x)\right)^T, \vec{\hat{v}}_L = (\hat{v}_{1L}, \hat{v}_{2L})^T,$$
$$\vec{\hat{w}}_L = (\hat{w}_{1L}, \hat{w}_{2L})^T, \vec{\hat{v}}_R = (\hat{v}_{1R}, \hat{v}_{2R})^T, \vec{\hat{w}}_R = (\hat{w}_{1R}, \hat{w}_{2R})^T.$$

The functions $\hat{u}_1(x), \hat{u}_2(x)$ are continuous ones and satisfy the reduced problem of (4)

$$\begin{cases} \hat{u}_1''(x) + \hat{u}_2(x) = 0, x \in \Omega, \\ b(x)\hat{u}_2(x) + \tilde{c}(x)\hat{u}_1(x) = f(x), x \in \bar{\Omega}, \\ \hat{u}_1(0) = p,\ \hat{u}_1(1) = q, \end{cases} \tag{9}$$

and

$$\vec{\hat{v}}_L = (\hat{v}_{1L}, \hat{v}_{2L})^T, \vec{\hat{v}}_R = (\hat{v}_{1R}, \hat{v}_{2R})^T$$

are the left layer corrections that defined as

$$\hat{v}_{1L}'' = -\hat{v}_{2L},\ \hat{v}_{2L} = \hat{k}_1 e^{-x\sqrt{\frac{b(0)}{\varepsilon}}},\ x \in \{0\} \cup \Omega^-,$$

$$\hat{v}_{1R}'' = -\hat{v}_{2R},\ \hat{v}_{2R} = \hat{k}_2 e^{-(x-d)\sqrt{\frac{b(d)}{\varepsilon}}},\ x \in \Omega^+ \cup \{1\},$$

while

$$\vec{\hat{w}}_L = (\hat{w}_{1L}, \hat{w}_{2L})^T, \vec{\hat{w}}_R = (\hat{w}_{1R}, \hat{w}_{2R})^T$$

are the right layer corrections that defined as

$$\hat{w}_{1L}'' = -\hat{w}_{2L},\ \hat{w}_{2L} = \hat{k}_3 e^{-(d-x)\sqrt{\frac{b(d)}{\varepsilon}}},\ x \in \{0\} \cup \Omega^-,$$

$$\hat{w}_{1R}'' = -\hat{w}_{2R}, \qquad \hat{w}_{2R} = \hat{k}_4 e^{-(1-x)\sqrt{\frac{b(1)}{\varepsilon}}}, \qquad x \in \Omega^+ \cup \{1\}.$$

The constants $\hat{k}_1, \hat{k}_2, \hat{k}_3$ and $\hat{k}_4$ are chosen such that $y_{2,as} \in C^0(\bar{\Omega}) \cap C^1(\Omega)$, that is,

$$\hat{y}_{2,as}(0) = \hat{y}_2(0),\ \hat{y}_{2,as}(1) = \hat{y}_2(1),$$

$$\hat{y}_{2,as}(d^+) = \hat{y}_{2,as}(d^-), \qquad \hat{y}'_{2,as}(d^+) = \hat{y}'_{2,as}(d^-).$$

The constants are given by [21,25]

$$\hat{k}_1 = [\hat{y}_2(0) - \hat{u}_2(0)] - \hat{k}_2 e^{-d\sqrt{\frac{b(d)}{\varepsilon}}},$$

$$\hat{k}_2 = \left(\frac{\hat{k}_{21}\left(\sqrt{b(d)} + \sqrt{b(1)}e^{-(1-d)\sqrt{\frac{b(d)+b(1)}{\varepsilon}}}\right)}{\hat{k}_{24}+\hat{k}_{25}} + \frac{(\hat{k}_{22}+\hat{k}_{23})\left(1-e^{\frac{-(1-d)\sqrt{(b(d)+b(0))}}{\varepsilon}}\right)}{\hat{k}_{24}+\hat{k}_{25}}\right),$$

$$\hat{k}_{21} = \left[\left(\hat{y}_2(1) - \hat{u}_2(1)\right)e^{-(1-d)\sqrt{\frac{b(1)}{\varepsilon}}} - \left(\hat{y}_2(0) - \hat{u}_2(0)\right)e^{-d\sqrt{\frac{b(0)}{\varepsilon}}}\right] + [\hat{u}_2(d+) - \hat{u}_2(d-)],$$

$$\hat{k}_{22} = \sqrt{b(1)}\left(\hat{y}_2(1) - \hat{u}_2(1)\right)e^{-(1-d)\sqrt{\frac{b(1)}{\varepsilon}}} + \sqrt{b(0)}(\hat{y}_2(0) - \hat{u}_2(0))e^{-d\sqrt{\frac{b(0)}{\varepsilon}}}],$$

$$\hat{k}_{23} = \sqrt{\varepsilon}[\hat{u}'_2(d+) - \hat{u}'_2(d-)],$$

$$\hat{k}_{24} = \left(\sqrt{b(d)} + \sqrt{b(1)}e^{-(1-d)\sqrt{\frac{b(1)+b(d)}{\varepsilon}}}\right)\left(1 - e^{-d\sqrt{\frac{b(0)+b(d)}{\varepsilon}}}\right),$$

$$\hat{k}_{25} = \left(\sqrt{b(d)} + \sqrt{b(0)}e^{-d\sqrt{\frac{b(0)+b(d)}{\varepsilon}}}\right)\left(1 - e^{-(1-d)\sqrt{\frac{b(1)+b(d)}{\varepsilon}}}\right),$$

$$\hat{k}_3 = \frac{\hat{k}_{31}+\hat{k}_{32}}{\hat{k}_{33}},$$

$$\hat{k}_{31} = [\hat{y}_2(0) - \hat{u}_2(0)]e^{-d\sqrt{\frac{b(0)}{\varepsilon}}} + \hat{k}_2\left(1 - e^{-d\sqrt{\frac{b(0)+b(d)}{\varepsilon}}}\right),$$

$$\hat{k}_{32} = [\hat{u}_2(d^+) - \hat{u}_2(d^-)] + [y_2(1) - \hat{u}_2(1)]e^{-(1-d)\sqrt{\frac{b(1)}{\varepsilon}}},$$

$$\hat{k}_{33} = \left(1 - e^{-(1-d)\sqrt{\frac{b(d)+b(1)}{\varepsilon}}}\right),$$

$$\hat{k}_4 = [\hat{y}_2(1) - \hat{u}_2(1)] - \hat{k}_3 e^{-(1-d)\sqrt{\frac{b(d)}{\varepsilon}}}.$$

Theorem 2.2. [21,23,25] The asymptotic expansion of zero-order, denoted as $\vec{\hat{y}}_{as}(x)$ as defined previously in (8) and (9) for the solution $\vec{\hat{y}}(x)$ of the SBVP (4) satisfies the inequality

$$\| \vec{\hat{y}}(x) - \vec{\hat{y}}_{as}(x) \|_{\infty} \leq C\sqrt{\varepsilon}, x \in \bar{\Omega}. \tag{10}$$

3. Piecewise analytical solution for the reduced problems (6) and (9)

To obtain approximate analytical solutions for SPBVPs (3) and (4) in a piecewise manner, we need only piecewise analytical solutions for the reduced problems (6) and (9). Substituting $u_2(x) = u_1'(x)$ from the first equation in (6) into the second one and defining the result equation on the left and right problem's domains, Ω^- and Ω^+, respectively, with initial and continuity conditions results in the following system of first-order IVPs:

$$\begin{cases} b(x)u_1'(x) + c(x)u_1(x) = f(x), x \in \Omega^-,\ u_1(0) = p, \\ b(x)u_1'(x) + c(x)u_1(x) = f(x), x \in \Omega^+, u_1(d^+) = u_1(d^-). \end{cases} \tag{11}$$

Finding the solution of the reduced problem (6) is equivalent to solving IVPs (11) and then getting $u_2(x)$ from the following equation:

$$u_2(x) = \frac{f(x)-c(x)u_1(x)}{b(x)}, x \in \bar{\Omega}. \tag{12}$$

Also, substituting $\hat{u}_2(x) = -\hat{u}_1''(x)$ from the first equation in (9) into the second one and defining the result equation on the left and right problem's domains, Ω^- and Ω^+, respectively, with terminal initial conditions results in the following system of second-order IVPs:

$$\begin{cases} -b(x)\hat{u}_1''(x) + \tilde{c}(x)\hat{u}_1(x) = f(x), x \in \Omega^-,\ \hat{u}_1(0) = p, \hat{u}'_1(0) = \alpha_1, \\ -b(x)\hat{u}_1''(x) + \tilde{c}(x)\hat{u}_1(x) = f(x), x \in \Omega^+, \hat{u}_1(1) = q, \hat{u}'_1(1) = \beta_1, \end{cases} \tag{13}$$

where α_1 and β_1 are unknown constants that can be determined from the continuity and smoothness conditions

$$\begin{cases} \hat{u}_1(d^+) = \hat{u}_1(d^-), \\ \hat{u}'_1(d^+) = \hat{u}'_1(d^-). \end{cases} \tag{14}$$

Finding the solution of the reduced problem (9) is equivalent to solving the second-order IVPs (13) and then getting $\hat{u}_2(x)$ from the following equation:

$$\hat{u}_2(x) = -\frac{f(x)-\tilde{c}(x)\hat{u}_1(x)}{b(x)}, x \in \bar{\Omega}. \tag{15}$$

3.1. RPSM for the reduced problems (11) and (13)

The RPSM consists of expressing the IVP solution as a power series expansion about the terminal point $x = x_0$ [33–35]. For solving the first-order IVPs (11), consider the following IVP:

$$b(x)u'(x) + c(x)u(x) - f(x) = 0, u(x_0) = \gamma, \tag{16}$$

and suppose that its solution takes the following form:

$$u(x) = \sum_{m=0}^{\infty} c_m(x - x_0)^m, \text{with } c_0 = \gamma, \tag{17}$$

and can be approximated by the following k^{th} truncated series:

$$u^k(x) = \sum_{m=0}^{k} c_m(x - x_0)^m. \tag{18}$$

Regarding applying the RPSM to IVP (16), the ∞^{th}-residual and k^{th}-residual functions are given, respectively, by

$$Res^{\infty}(x) = b(x)\sum_{m=1}^{\infty} mc_m(x - x_0)^{m-1} + c(x)\sum_{m=0}^{\infty} c_m(x - x_0)^m - f(x) = 0, \tag{19}$$

$$Res^{k}(x) = b(x)\sum_{m=1}^{k} mc_m(x - x_0)^{m-1} + c(x)\sum_{m=0}^{k} c_m(x - x_0)^m - f(x) = 0. \tag{20}$$

It is evident that the function $Res^{\infty}(x)$ is infinitely differentiable at $x = x_0$. Moreover,

$$\frac{d^{\bar{n}}}{dx^{\bar{n}}}Res^{\infty}(x_0) = \frac{d^{\bar{n}}}{dx^{\bar{n}}}Res^{k}(x_0), \ \bar{n} = 1,2,\ldots,k, \tag{21}$$

which is a fundamental rule in the RPSM. Using (21), we can determine the unknowns $c_m, m = 1..k$ and the approximate residual power series solution $u^k(x)$ is obtained. For solving the second-order IVPs (13), consider the following second-order IVP:

$$-b(x)\hat{u}''(x) + \tilde{c}(x)\hat{u}(x) - f(x) = 0, \hat{u}(x_0) = \gamma_1, \ \hat{u}'(x_0) = \delta_1, \tag{22}$$

and suppose that its k-$^{\text{th}}$ truncated series solution takes the following form:

$$\hat{u}^k(x) = \sum_{m=0}^{k} c_m(x - x_0)^m, \text{with } c_0 = \gamma_1, c_1 = \delta_1. \tag{23}$$

The k^{th}-residual function is given by

$$Res^{k}(x) = -b(x)\sum_{m=2}^{k} m(m-1)c_m(x - x_0)^{m-2} + \tilde{c}(x)\sum_{m=0}^{k} c_m(x - x_0)^m - f(x). \tag{24}$$

Using the same procedure by applying the basic rule in the RPSM on (24), the approximate residual power series solution $\hat{u}^k(x)$ is obtained.

3.2. Padé approximant $\left[\frac{l}{n}\right]$ *at* $x = x_0$

To enhance the accuracy of the series solution obtained from the RPSM, we recommend employing the Padé approximation for the truncated series solution (23). We assume that the solution of the reduced problems (11), (13) and its corresponding series expansion (23) satisfy the conditions

of Padé approximant [37,41].

Let the rational approximation of the truncated series solution $u^k(x)$ or $\hat{u}^k(x)$ defined by (18) and (23), respectively, is the quotient of two polynomials $P_l(x)$ and $Q_n(x)$ of degree l and n respectively and defined by

$$u^{\left[\frac{l}{n}\right]}(x) = \frac{P_l(x)}{Q_n(x)},\ l+n \le k, \tag{25}$$

where

$$P_l(x) = \sum_{r=0}^{l} p_r(x-x_0)^r\,, Q_n(x) = \sum_{r=0}^{n} q_r(x-x_0)^r, q_0 = 1. \tag{26}$$

The polynomials in (26) are constructed to ensure that $u(x)$ and $u^{\left[\frac{l}{n}\right]}(x)$ agree at $x = x_0$ and their derivatives up to the order $l+n \le k$. Then the formal power series

$$u(x) - \frac{P_l(x)}{Q_n(x)} = O((x-x_0)^{l+n+1}) \tag{27}$$

determines the coefficients of $P_l(x)$ and $Q_n(x)$. Multiplying (27) by $Q_n(x)$ results in

$$\left(\sum_{m=0}^{\infty} c_m(x-x_0)^m\right)\left(\sum_{r=0}^{n} q_r(x-x_0)^r\right) - \left(\sum_{r=0}^{l} p_r(x-x_0)^r\right) = \sum_{r=l+n+1}^{\infty} c_r(x-x_0)^r. \tag{28}$$

Expanding the left side of Eq (28) and equating the coefficients of the powers of $(x-x_0)^r$ to zero for $r = 0,1,\ldots,l+n$ yields a system of $2(l+n+1)$ linear equations in the $2(l+n+1)$ unknown coefficients of $P_l(x)$ and $Q_n(x)$. By solving this linear system, we obtain the rational approximation $u^{\left[\frac{l}{n}\right]}(x)$. Although Padé approximation $u_i^{\left[\frac{l}{n}\right]}(x)$ agrees with truncated Taylor expansions $\hat{u}^{l+n}(x)$ up to order $O(l+m)$, Padé approximation can outperform truncated Taylor expansion because it can accurately represent functions with poles or singularities outside the region of convergence of a Taylor expansion, resulting in more accurate and stable approximation [37,41].

The piecewise approximate analytical solutions for Eqs (3) and (4) are obtained and given by, respectively,

$$\begin{cases} y_{1,ap}^k = u_1^{\left[\frac{l}{n}\right]} + \vec{v}_L + \vec{w}_L,\ x \in \Omega^- \cup \{0, \mathrm{d}\}, \\ y_{2,ap}^k = u_2^{\left[\frac{l}{n}\right]} + \vec{v}_R + \vec{w}_R,\ x \in \Omega^+ \cup \{1\}, \end{cases} \tag{29}$$

where

$$\vec{y}_{ap} = \left(y_{1,ap}^k, y_{2,ap}^k\right)^T, \vec{u}^{[l,n]} = \left(u_1^{\left[\frac{l}{n}\right]}, u_2^{\left[\frac{l}{n}\right]}\right)^T$$

and

$$\begin{cases} \hat{y}_{1,ap}^k = \hat{u}_1^{\left[\frac{l}{n}\right]} + \vec{\hat{v}}_L + \vec{\hat{w}}_L,\ x \in \Omega^- \cup \{0, \mathrm{d}\}, \\ \hat{y}_{2,ap}^k = \hat{u}_2^{\left[\frac{l}{n}\right]} + \vec{\hat{v}}_R + \vec{\hat{w}}_R,\ x \in \Omega^+ \cup \{1\}, \end{cases} \tag{30}$$

where

$$\vec{\hat{y}}_{ap} = \left(\hat{y}_{1,ap}^k, \hat{y}_{2,ap}^k\right)^T, \vec{\hat{u}}^{[l,n]} = \left(\hat{u}_1^{\left[\frac{l}{n}\right]}, \hat{u}_2^{\left[\frac{l}{n}\right]}\right)^T.$$

4. Error estimate of the method

The numerical error in the current method arises from two sources: one originating from the asymptotic approximation and the other from the analytical approximation using the RPSPM.

Theorem 4.1. *The solution*

$$\vec{y}(x) = \left(y_1(x), y_2(x) \right)^T$$

of (3) and the approximate analytical solution

$$\vec{y}_{ap}(x) = \left(y_{1,ap}^k(x), y_{2,ap}^k(x) \right)^T$$

in (29) satisfy the inequality

$$\| \vec{y}(x) - \vec{y}_{ap}(x) \|_\infty \leq \mathrm{C} \left(\varepsilon + \frac{1}{(l+n+1)!} \right).$$

Proof. We have

$$\| \vec{y}(x) - \vec{y}_{ap}(x) \|_\infty \leq \| \vec{y}(x) - \vec{y}_{as}(x) \|_\infty + \| \vec{y}_{as}(x) - \vec{y}_{ap}(x) \|_\infty$$

and

$$\| \vec{y}_{as}(x) - \vec{y}_{ap}(x) \|_\infty \leq \left\| \vec{u}(x) - \vec{u}^{\left[\frac{l}{n}\right]}(x) \right\|_\infty .$$

And since Padé approximant $\vec{u}^{[l,n]}(x)$ has a bounded error given by [37,41]

$$\left\| \vec{u}(x) - \vec{u}^{\left[\frac{l}{n}\right]}(x) \right\|_\infty \leq \frac{T}{(l+n+1)!}, T \leq \left\| u^{(l+n+1)}(\pi_1) \right\|, \ 0 \leq \pi_1 \leq 1.$$

Therefore, utilizing Theorem 2.1 and the aforementioned bounded errors, we can conclude that

$$\| \vec{y}(x) - \vec{y}_{ap}(x) \|_\infty \leq \mathrm{C} \left(\sqrt{\varepsilon} + \frac{1}{(l+n+1)!} \right).$$

Remark 4.1. A similar statement is true for the SPBVS (4) and (30).

5. Numerical results and discussion

This section presents numerical examples to demonstrate the method's accuracy and efficiency. These examples have been carefully selected from the literature, where they have been solved using other numerical methods in literature and have known exact solutions. This allows for a comprehensive comparison of the results. All Symbolic calculations were performed using Maple 14, while numerical simulations and figures were generated using MATLAB 2017b. The computations were performed on a laptop with an Intel Core i7G processor and 8 GB of RAM. Algorithms 1 and 2 present the pseudocode for the proposed method applied to SPBVPs (3) and (4), respectively, demonstrating its use in obtaining numerical results.

Algorithm 1. For third-order SPBVP (1).

Input:

Define

- Coefficients of the differential equation: $b(x), c(x), f(x)$.
- Boundary conditions: p, d.
- Order of series expansion: N.

Steps

1) Solve the IVP (11) for the left interval using RPSM.
2) Evaluate the solution at the boundary condition d.
3) Solve the IVP (11) for the right interval with the boundary condition from step 2.
4) Apply the Padé approximation to the left and right obtained solutions from steps 1 and 3.
5) Construct the approximate solutions $\vec{y}_{ap}$ as given in (29).

Output

Approximate solution: $\vec{y}_{ap}$

and

Algorithm 2. For fourth-order SPBVP (2).

Input:

Define

- Coefficients of the differential equation: $b(x), \tilde{c}(x), f(x)$.
- Boundary conditions: p, q, d.
- Order of series expansion: N.

Steps

1) Solve the IVP (13) for the left interval using RPSM.
2) Solve the IVP (13) for the right interval using RPSM.
3) Construct two equations as given in (14) using series approximations from steps 1 and 2 and their derivative at $x = d$.
4) Solve the equations in step 3 for $\alpha_1$and β_1.
5) Apply the Padé approximation to the left and right obtained solutions from steps 1 and 2.
6) Construct the approximate solutions $\vec{y}_{ap}$ as given in (30).

Output

Approximate solution: $\vec{y}_{ap}$

Example 1. Consider the following third-order SPBVP with constant coefficients [22,23,25]:

$$-\varepsilon y'''(x) + 4y'(x) - y(x) = f(x), \quad x \in (\Omega^- \cup \Omega^+), \tag{31}$$

where

$$f(x) = \begin{cases} 0.7, & 0 \le x \le 0.5, \\ -0.6, & 0.5 < x \le 1, \end{cases}$$

and

$$y(0) = 1\,,\ y'(0) = 0,\ \ y'(1) = 0. \tag{32}$$

By employing the 8^{th}-order RPSPM, the piecewise approximate analytical solution is given by:

$$y_{1,ap}^{8}=\begin{cases}\dfrac{1.00+6.70\times10^{-3}x^{2}+300.00\times10^{-3}x+446.00\times10^{-6}x^{3}+2.33\times10^{-6}x^{4}}{1.00+6.70\times10^{-3}x^{2}-125.00\times10^{-3}x-186.00\times10^{-6}x^{3}+2.33\times10^{-6}x^{4}}-\dfrac{\sqrt{\varepsilon}}{2}\left(k_{1}\mathrm{e}^{\frac{-2x}{\sqrt{\varepsilon}}}-k_{3}\mathrm{e}^{\frac{x-1}{\sqrt{\varepsilon}}}\right),\\ 0\le x\le 0.5,\\ \dfrac{1.35-36.03\times10^{-3}x+8.31\times10^{-3}(x-1)^{2}-290.00\times10^{-6}(x-1)^{3}+2.81\times10^{-6}(x-1)^{4}}{1.16-162.99\times10^{-3}x+11.49\times10^{-3}(x-1)^{2}-429.09\times10^{-6}(x-1)^{3}+7.51\times10^{-6}(x-1)^{4}}-\dfrac{\sqrt{\varepsilon}}{2}\left(k_{2}\mathrm{e}^{\frac{1-2x}{\sqrt{\varepsilon}}}+k_{4}\mathrm{e}^{\frac{2x-2}{\sqrt{\varepsilon}}}\right),\\ 0.5<x\le 1,\end{cases}$$

$$y_{2,ap}^{8}=\begin{cases}\dfrac{425.00\times10^{-3}+53.12\times10^{-3}x+2.85\times10^{-3}x^{2}+79.05\times10^{-6}x^{3}+988.19\times10^{-9}x^{4}}{1.0000-125.00\times10^{-3}x+6.70\times10^{-3}x^{2}-186.01\times10^{-6}x^{3}+2.32\times10^{-6}x^{4}}-\dfrac{1}{2}\left(-2k_{1}\mathrm{e}^{\frac{-2x}{\sqrt{\varepsilon}}}+k_{3}\mathrm{e}^{\frac{x-1}{\sqrt{\varepsilon}}}\right),\\ 0\le x\le 0.5,\\ \dfrac{162.00\times10^{-3}+15.44\times10^{-3}x+353.64\times10^{-6}(x-1)^{2}-8.14\times10^{-6}(x-1)^{3}-424.93\times10^{-9}(x-1)^{4}}{1.1630-162.99\times10^{-3}x+11.49\times10^{-3}(x-1)^{2}-429.09\times10^{-6}(x-1)^{3}+7.51\times10^{-6}(x-1)^{4}}+\left(k_{2}\mathrm{e}^{\frac{1-2x}{\sqrt{\varepsilon}}}-k_{4}\mathrm{e}^{\frac{2x-2}{\sqrt{\varepsilon}}}\right),\\ 0.5<x\le 1,\end{cases}$$

where

$$\pi_{1}=e^{\frac{-4}{\sqrt{\varepsilon}}}-1,$$

$$k_{1}=\left(-0.16249+0.020313\sqrt{\varepsilon}\right)\mathrm{e}^{\frac{-3}{\sqrt{\varepsilon}}}+\left(-0.16249-0.020313\sqrt{\varepsilon}\right)\mathrm{e}^{\frac{-1}{\sqrt{\varepsilon}}}+0.42500-0.17744\mathrm{e}^{\frac{-2}{\sqrt{\varepsilon}}},$$

$$k_{2}=\left(-0.16249-0.020313\sqrt{\varepsilon}\right)\mathrm{e}^{\frac{-2}{\sqrt{\varepsilon}}}-0.16249+0.42500\mathrm{e}^{\frac{-1}{\sqrt{\varepsilon}}}-0.17744\mathrm{e}^{\frac{-3}{\sqrt{\varepsilon}}}+0.020313\sqrt{\varepsilon},$$

$$k_{3}=\left(0.16249-0.020313\sqrt{\varepsilon}\right)\mathrm{e}^{\frac{-2}{\sqrt{\varepsilon}}}+0.16249+0.17744\mathrm{e}^{\frac{-1}{\sqrt{\varepsilon}}}-0.42499\mathrm{e}^{\frac{-3}{\sqrt{\varepsilon}}}+0.020313\sqrt{\varepsilon},$$

$$k_{4}=\left(0.16249+0.020313\sqrt{\varepsilon}\right)\mathrm{e}^{\frac{-3}{\sqrt{\varepsilon}}}+\left(0.16249-0.020313\sqrt{\varepsilon}\right)\mathrm{e}^{\frac{-1}{\sqrt{\varepsilon}}}+0.17744-0.42499\mathrm{e}^{\frac{-2}{\sqrt{\varepsilon}}}.$$

Figure 1 illustrates the profile of the approximate first derivative solution of Example 1 at $k=8$, considering various values of ε. In Figure 2, the distribution of the pointwise residual error is shown over the entire problem's domain, and a specific interior region that includes the internal layer. The pointwise residual error, denoted as Er, is defined as

$$Er=Eres_{\varepsilon}^{k}(x_{i})=\left|\varepsilon\frac{d^{\bar{n}}}{dx^{\bar{n}}}y_{1,ap}^{k}(x_{i})+b(x_{i})\frac{d^{\bar{n}-2}}{dx^{\bar{n}-2}}y_{1,ap}^{k}(x_{i})+c(x_{i})y_{1,ap}^{k}(x_{i})-f(x_{i})\right|,x_{i}\in[0,1],$$

where $\bar{n}=3,4$ for the third and fourth-order SPBVP, respectively.

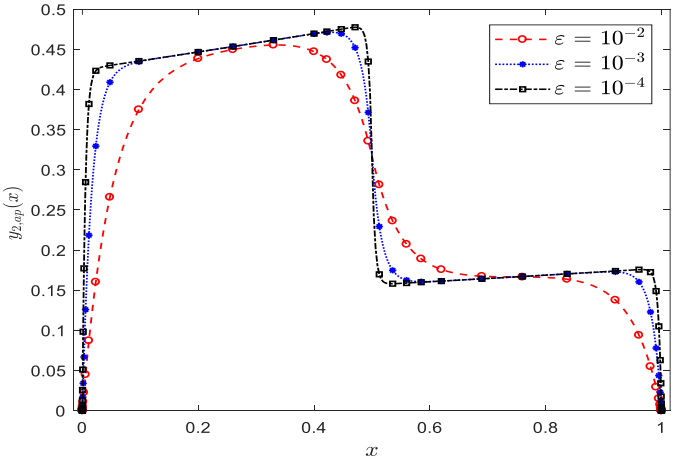

Figure 1. Approximate solution profile for the first derivative in Example 1 at $k=8$ for various values of ε.

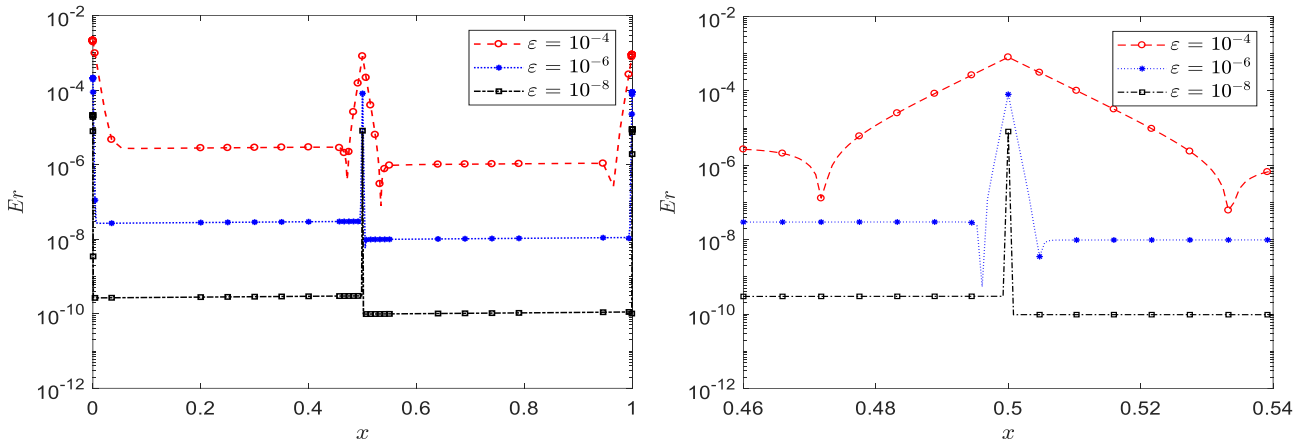

Figure 2. The pointwise residual error for the first derivative of Example 1 at $k = 8$ over (left) problem's domain and (right) the interior region, for various values of ε.

Figure 3 depicts the distribution of the error over the left and right boundary regions using a logarithmic scale. Figures 1–3 show that decreasing ε improves the solution accuracy. Moreover, the numerical results validate that the method yields accurate solutions not only over the outer regions but also within the interior and boundary layer regions.

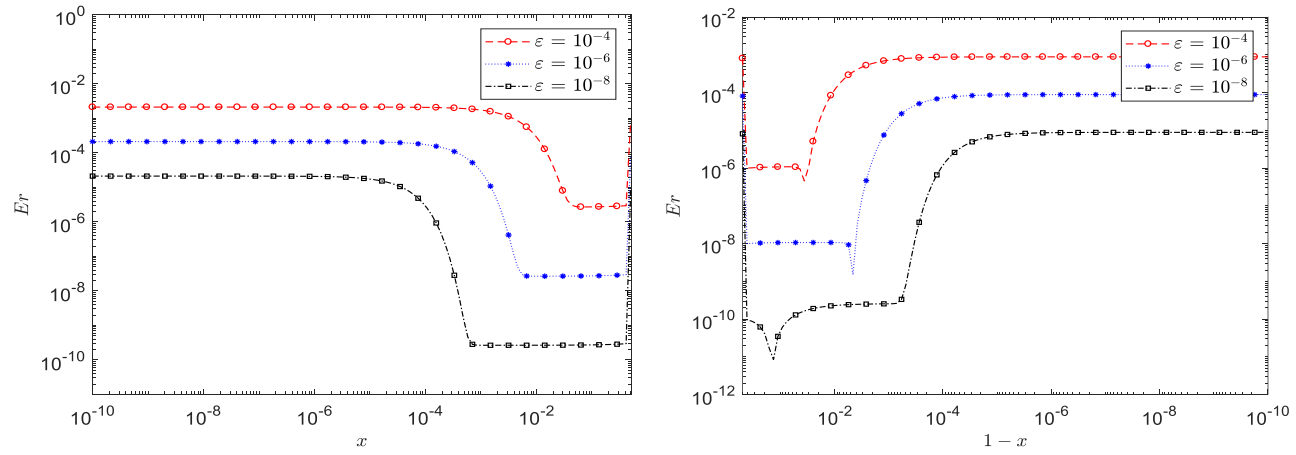

Figure 3. The pointwise residual error for the first derivative of Example 1 at $k = 8$ over (left) the left region and (right) the right region, for various values of ε.

Table 1 summarizes the maximum residual error

$$Er_{max} = \max_{0 \le x_i \le 1} Eres_{\varepsilon}^{k}(x_i),$$

and the CPU computational time required for solving Example 1 using the RPSM and RPSPM methods. It presents the results obtained for varying values of ε and k. In Tables 2–4, a comparison of the maximum pointwise error in the first derivative solution is presented. This comparison includes the results obtained using the present method and three other asymptotic numerical methods: the finite difference method [22], the finite element method [23], and the hybrid difference scheme [25]. Since the double mesh principle is not applicable here, the maximum pointwise error is computed as

$$E_{max}^{k} = \max_{0\le x_i\le 1} \left| y_{2,ap}^{100}(x_i) - y_{2,ap}^{k}(x_i) \right|.$$

Results in [23,25] are specifically presented for $\varepsilon = 10^{-16}$ and $\varepsilon = 2^{-1}-2^{-31}$, respectively, using different numbers of grid points. Notably, both studies achieved the highest accuracy when employing 1024 grid points. As a result, Tables 3 and 4 exclusively present these specific results to enable a meaningful comparison between the methods. The numerical results clearly demonstrate that the proposed method achieves higher accuracy compared to other numerical methods available in the literature, even when utilizing a smaller number of RPSPM terms.

Table 1. Maximum residual error ER_{ε}^{N} for Example 1 using RPSM and RPSPM at different values of ε.

ε	RPSM			RPSPM		
	$k=4$	$k=6$	$k=8$	$k=4$	$k=6$	$k=8$
10^{-1}	6.748971E-02	6.748964E-02	6.748964E-02	6.748965E-02	6.748964E-02	6.748964E-02
10^{-3}	6.746403E-03	6.746403E-03	6.746403E-03	6.746403E-03	6.746403E-03	6.746403E-03
10^{-5}	6.722496E-04	6.722496E-04	6.722496E-04	6.722496E-04	6.722496E-04	6.722496E-04
10^{-7}	6.720106E-04	6.720106E-05	6.720106E-05	6.720106E-05	6.720106E-05	6.720106E-05
10^{-9}	1.472400E-04	6.719867E-06	6.719867E-06	6.719867E-06	6.719867E-06	6.719867E-06
10^{-11}	1.703636E-04	6.719843E-07	6.719843E-07	3.013296E-06	6.719843E-07	6.719843E-07
10^{-13}	1.726760E-04	6.719840E-08	6.719840E-08	3.244537E-06	6.719840E-08	6.719840E-08
10^{-15}	1.729072E-04	6.719840E-08	6.719840E-09	3.267661E-06	6.719840E-09	6.719840E-09
10^{-17}	1.729304E-04	8.749989E-08	6.719840E-10	3.269974E-06	7.676429E-10	6.719840E-10
10^{-19}	1.729327E-04	8.981231E-08	6.719840E-11	3.270205E-06	5.364014E-10	6.719840E-11
10^{-21}	1.729329E-04	9.004355E-08	6.719840E-11	3.270228E-06	5.132772E-10	6.719840E-12
10^{-23}	1.729329E-04	9.006667E-08	2.256158E-11	3.270230E-06	5.109648E-10	6.719840E-13
10^{-25}	1.729329E-04	9.006898E-08	2.487399E-11	3.270231E-06	5.107336E-10	6.978750E-14
10^{-31}	1.729329E-04	9.006924E-08	2.513067E-11	3.270231E-06	5.107079E-10	4.259023E-14
CPU time (sec)	0.093	0.094	0.102	0.096	0.101	0.103

Table 2. Maximum pointwise error for Example 1 at different values of ε.

ε	Finite difference method [22] (1024 points)	Present method E_{max}^{k}		
		$k=4$	$k=6$	$k=8$
2^{-4}	4.64790E-05	2.681968E-08	1.185786E-10	7.039917E-15
2^{-6}	1.57036E-05	6.797518E-08	6.475628E-11	7.555520E-16
2^{-8}	1.47904E-05	1.010479E-07	1.638425E-10	4.425946E-15
2^{-10}	2.38508E-05	1.173066E-07	2.135268E-10	7.056056E-15
2^{-20}	6.94328E-05	1.330571E-07	2.616585E-10	9.604001E-15
2^{-30}	6.94319E-05	1.335493E-07	2.631626E-10	9.683625E-15
2^{-40}	6.94320E-05	1.335647E-07	2.632096E-10	9.686113E-15

Table 3. Maximum pointwise error for Example 1 at $\varepsilon = 10^{-16}$.

Finite element method [23] (1024 points)		Present method E_{max}^{k}		
Shishkin mesh	Bakhavlov-Shishkin mesh	$k=4$	$k=6$	$k=8$
2.9542E-04	9.4492E-07	1.335300E-07	2.632111E-10	9.686192E-15

Table 4. Maximum pointwise error for Example 1 at $\varepsilon = 2^{-1}-2^{-31}$.

Hybrid difference scheme [25] (1024 points)	Present method E_{max}^{k}		
	$k=4$	$k=6$	$k=8$
3.9850E-4	5.735978E-07	5.422338E-10	1.073623E-14

Example 2. Consider the following third-order SPBVP with variable coefficients [22]:

$$-\varepsilon y'''(x) + (1+x)y'(x) - y(x) = f(x), \quad x \in (\Omega^- \cup \Omega^+), \tag{33}$$

where

$$f(x) = \begin{cases} x \ , & 0 \le x \le 0.5, \\ (1+x)^2, & 0.5 < x \le 1, \end{cases}$$

and

$$y(0) = 1\,,\ y'(0) = 1,\ y'(1) = 0. \tag{34}$$

By employing the 8^{th}-order RPSPM, the piecewise approximate analytical solution is given by:

$$y_{1,ap}^{8} = \begin{cases} \dfrac{1 + 1.8667x + 1.5571x^2 + 7.7143\times10^{-1}x^3 + 1.5540\times10^{-1}x^4}{1 + 1.8667x + 1.0571x^2 + 1.7143\times10^{-1}x^3 - 9.5240\times10^{-4}x^4} - \pi_2\sqrt{\varepsilon}\left(k_1 e^{\frac{-x}{\sqrt{\varepsilon}}} - \sqrt{\frac{2}{3}}k_3 e^{\frac{2x-1}{4\sqrt{\varepsilon/6}}}\right), & 0 \le x \le 0.5, \\ 0.4695 + x + 0.5x^2 - \pi_2\sqrt{\varepsilon}\left(\sqrt{\frac{2}{3}}k_2 e^{\frac{2x-1}{4\sqrt{\varepsilon/6}}} - \frac{1}{\sqrt{2}}k_4 e^{\frac{x-1}{\sqrt{\varepsilon/2}}}\right), & 0.5 < x \le 1, \end{cases}$$

$$y_{2,ap}^{8} = \begin{cases} \dfrac{x}{1+x} + \pi_2\left(k_1 e^{\frac{-x}{\sqrt{\varepsilon}}} + k_3 e^{\frac{2x-1}{4\sqrt{\varepsilon/6}}}\right), & 0 \le x \le 0.5, \\ 1 + x + \pi_2\left(-k_2 e^{\frac{2x-1}{4\sqrt{\varepsilon/6}}} + k_4 e^{\frac{x-1}{\sqrt{\varepsilon/2}}}\right), & 0.5 < x \le 1, \end{cases}$$

where

$$\pi_2 = \left(48284.\,e^{\frac{2.4319}{\sqrt{\varepsilon}}} - 3789.\,e^{\frac{-1.3195}{\sqrt{\varepsilon}}} + 4495.\,e^{\frac{-1.1124}{\varepsilon}} - 48990\right)^{-1},$$

$$k_1 = \left(-1.1111\sqrt{\varepsilon} + 3.2998\right)e^{-\frac{1.9319}{\sqrt{\varepsilon}}} - 10.935e^{-\frac{1.3195}{\sqrt{\varepsilon}}} - 4.89 + \left(1.1111\sqrt{\varepsilon} + 2.8578.\right)e^{-\frac{0.61238}{\sqrt{\varepsilon}}},$$

$$k_2 = \left(2.3334 + 1.1111\sqrt{\varepsilon}\right)e^{-\frac{1.1124}{\sqrt{\varepsilon}}} + 0.75767e^{-\frac{0.70710}{\sqrt{\varepsilon}}} - 9.6567e^{-\frac{1.8195}{\sqrt{\varepsilon}}} + 2.857 - 4.4495e^{-\frac{0.50000}{\sqrt{\varepsilon}}} - 1.1111\sqrt{\varepsilon},$$

$$k_3 = \left(5.5555\sqrt{\varepsilon} - 16.499\right)e^{-\frac{1.3195}{\sqrt{\varepsilon}}} + 24.142e^{-\frac{1.8195}{\sqrt{\varepsilon}}} + 2.2475e^{-\frac{0.50000}{\sqrt{\varepsilon}}} - 14.289 - 5.5555\sqrt{\varepsilon} + 52.78e^{-\frac{0.70710}{\sqrt{\varepsilon}}},$$

$$k_4 = \left(-2.3334 - 1.1111\sqrt{\varepsilon}\right)e^{-\frac{1.7248}{\sqrt{\varepsilon}}} + 3.5505e^{-\frac{1.1124}{\sqrt{\varepsilon}}} + 9.7979 + \left(-2.8578 + 1.1111\sqrt{\varepsilon}\right)e^{-\frac{0.61238}{\sqrt{\varepsilon}}}.$$

Figure 4 depicts the profile of the approximate first derivative solution of Example 2 at $k = 8$ for different values of ε. In Figure 5, the distribution of the pointwise residual error, Er, is shown over the entire problem's domain and the interior layer region. Furthermore, Figure 6 presents this error distribution over the left and right boundary regions. The results from Figures 5 and 6 validate that the method yields accurate solutions not only in the outer regions but also within the interior and boundary layer regions.

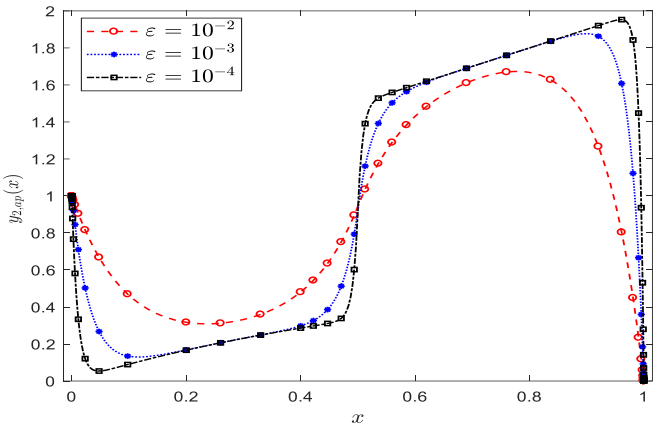

Figure 4. Approximate solution profile for the first derivative solution of Example 2 at $k = 8$, for various values of ε.

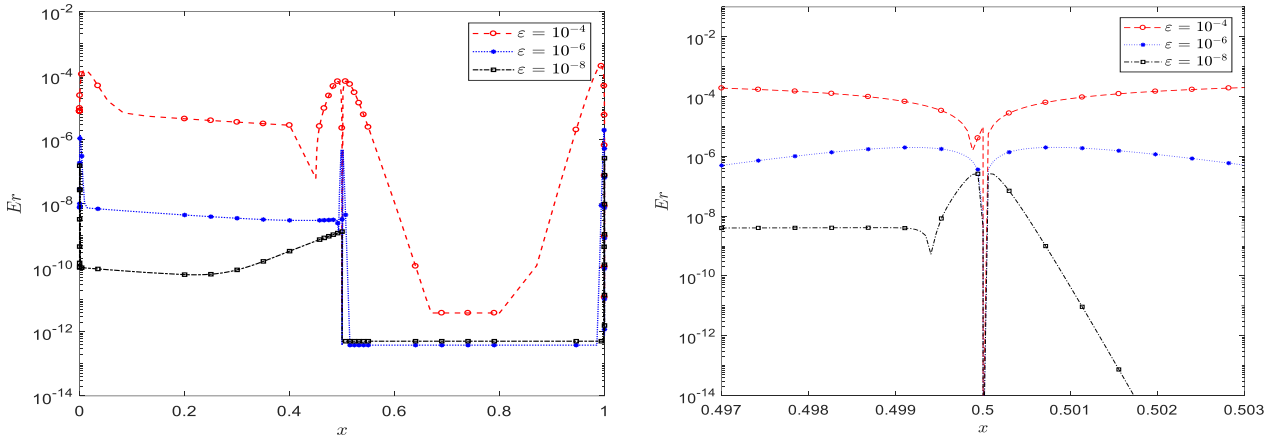

Figure 5. The pointwise residual error for the first derivative of Example 2 at $k = 8$ over (left) problem's domain and (right) the interior region, for various values of ε.

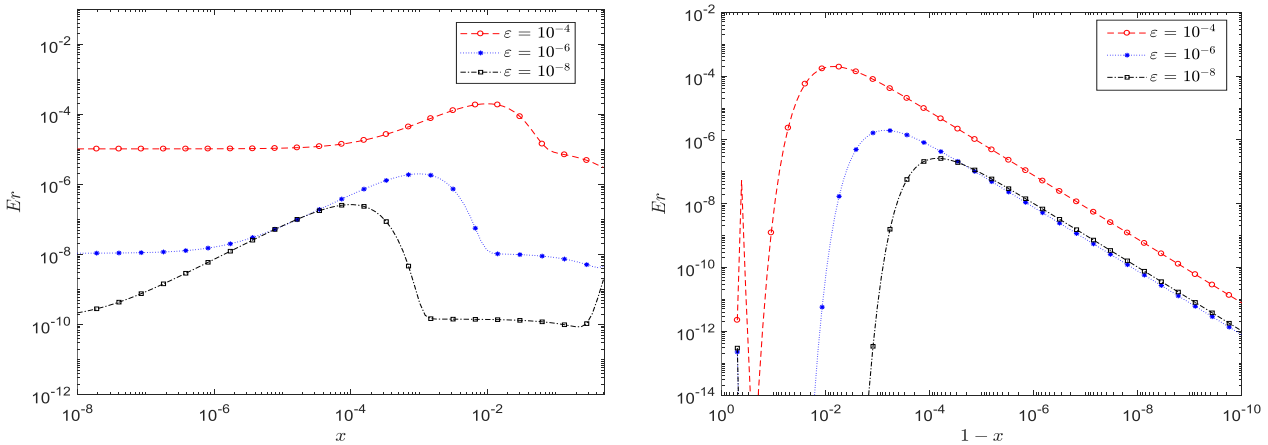

Figure 6. The pointwise residual error for the first derivative of Example 2 at $k = 8$ over (left) the left region and (right) the right region, for various values of ε.

Table 5 summarizes the maximum residual error, Er_{max}, and the CPU computational time required for solving Example 2 using the RPSM and RPSPM methods. It presents the results obtained for varying values of ε and k. Table 6 compares the maximum pointwise error in the first derivative solution between the present method and the asymptotic finite difference method in [22]. The numerical results clearly demonstrate that the proposed method achieves higher accuracy compared to the results obtained in [22].

Table 5. Maximum residual error ER_{ε}^{N} for Example 2 using RPSM and RPSPM at different values of ε.

ε	RPSM			RPSPM		
	$k=4$	$k=6$	$k=8$	$k=4$	$k=6$	$k=8$
10^{-1}	1.745691E-01	1.716983E-01	1.706936E-01	1.703964E-01	1.702331E-01	1.702312E-01
10^{-2}	5.586477E-02	1.934999E-02	1.934222E-02	1.934045E-02	1.933902E-02	1.933901E-02
10^{-3}	6.150007E-02	1.512507E-02	3.968818E-03	3.152192E-03	1.999999E-03	1.999999E-03
10^{-4}	6.240000E-02	1.557500E-02	3.912500E-03	2.658703E-03	2.000000E-04	2.000000E-04
10^{-5}	6.249000E-02	1.562000E-02	3.906875E-03	2.609361E-03	2.975291E-05	2.000000E-05
10^{-6}	6.249900E-02	1.562450E-02	3.906313E-03	2.604426E-03	2.442899E-05	2.000000E-06
10^{-7}	6.249990E-02	1.562495E-02	3.906256E-03	2.603933E-03	2.389660E-05	3.179415E-07
10^{-8}	6.249999E-02	1.562499E-02	3.906251E-03	2.603884E-03	2.384336E-05	2.646102E-07
10^{-9}	6.250000E-02	1.562500E-02	3.906250E-03	2.603879E-03	2.383804E-05	2.592771E-07
10^{-10}	6.250000E-02	1.562500E-02	3.906250E-03	2.603878E-03	2.383750E-05	2.587437E-07
10^{-20}	6.250000E-02	1.562500E-02	3.906250E-03	2.603878E-03	2.383745E-05	2.586845E-07
10^{-30}	6.250000E-02	1.562500E-02	3.906250E-03	2.603878E-03	2.383745E-05	2.586845E-07
CPU time (sec)	0.101	0.101	0.105	0.102	0.103	0.110

Table 6. Maximum pointwise error for Example 2 at different values of ε.

ε	Finite difference method [22] (1024 points)	Present method E_{max}^{k}			
		$k=4$	$k=6$	$k=8$	$k=10$
2^{-4}	3.49375E-06	2.371451E-04	7.016900E-06	1.307000E-07	1.900000E-09
2^{-6}	1.21228E-04	3.043280E-04	3.246000E-07	2.460000E-08	1.541000E-09
2^{-8}	1.31797E-04	5.860590E-04	4.133800E-06	3.150000E-08	1.468670E-09
2^{-10}	1.35090E-04	7.270097E-04	6.040300E-06	5.980000E-08	1.977100E-09
2^{-20}	6.50928E-04	8.635546E-04	7.886500E-06	8.630000E-08	1.800000E-09
2^{-30}	6.50655E-04	8.678218E-04	7.944000E-06	8.720000E-08	1.800000E-09
2^{-34}	6.50647E-04	8.679251e-04	7.945600e-06	8.740000e-08	1.800000E-09

Example 3. Consider the following fourth-order SPBVP [21,23,25,27]:

$$-\varepsilon y^{(iv)}(x) + 4y''(x) + y(x) = f(x), \quad x \in (\Omega^- \cup \Omega^+), \tag{35}$$

where

$$f(x) = \begin{cases} 0.7, & 0 \le x \le 0.5, \\ -0.6, & 0.5 < x \le 1, \end{cases}$$

and

$$y(0) = y(1) = 1\,,\ y''(0) = y''(1) = 0. \tag{36}$$

By employing the 8^{th}-order RPSPM, the piecewise approximate analytical solution is given by

$$y_{1,ap}^{8}=\begin{cases}\dfrac{1.00-160.09\times10^{-3}x+200.20\times10^{-3}x^{2}-3.41\times10^{-3}x^{3}+2.14\times10^{-3}x^{4}}{1.00+8.91\times10^{-3}x-10.79\times10^{-3}x^{2}-87.71\times10^{-6}x^{3}+52.06\times10^{-6}x^{4}}+\dfrac{\varepsilon}{4}\left(k_{1}e^{\frac{-2}{\sqrt{\varepsilon}}}-k_{3}e^{\frac{2x-1}{\sqrt{\varepsilon}}}\right), & 0\le x\le 0.5,\\ \dfrac{933.89\times10^{-3}+66.11\times10^{-3}x+37.79\times10^{-3}(x-1)^{2}+1.88\times10^{-3}(x-1)^{3}+511.08\times10^{-6}(x-1)^{4}}{1.02-22.06\times10^{-3}x-10.26\times10^{-3}(x-1)^{2}+216.75\times10^{-6}(x-1)^{3}+44.57\times10^{-6}(x-1)^{4}}-\dfrac{\varepsilon}{4}\left(k_{2}e^{\frac{1-2x}{\sqrt{\varepsilon}}}+k_{4}e^{\frac{2x-2}{\sqrt{\varepsilon}}}\right), & 0.5<x\le 1,\end{cases}$$

$$y_{2,ap}^{8}=\begin{cases}\dfrac{425.00\times10^{-3}-38.46\times10^{-3}x+48.16\times10^{-3}x^{2}-868.25\times10^{-6}x^{3}+543.44\times10^{-6}x^{4}}{1.00+8.91\times10^{-3}x-10.79\times10^{-3}x^{2}-87.71\times10^{-6}x^{3}+52.06\times10^{-6}x^{4}}-\left(k_{1}e^{\frac{-2}{\sqrt{\varepsilon}}}-k_{3}e^{\frac{2x-1}{\sqrt{\varepsilon}}}\right), & 0\le x\le 0.5,\\ \dfrac{80.16\times10^{-3}+19.84\times10^{-3}x+10.99\times10^{-3}(x-1)^{2}+438.09\times10^{-6}(x-1)^{3}+121.08\times10^{-6}(x-1)^{4}}{1.02-22.06\times10^{-3}x-10.26\times10^{-3}(x-1)^{2}+216.75\times10^{-6}(x-1)^{3}+44.57\times10^{-6}(x-1)^{4}}-\left(k_{2}e^{\frac{1-2x}{\sqrt{\varepsilon}}}+k_{4}e^{\frac{2x-2}{\sqrt{\varepsilon}}}\right), & 0.5<x\le 1,\end{cases}$$

where

$$k_{1}=\left(0.16317-1.87\times10^{-12}\sqrt{\varepsilon}\right)e^{\frac{-3}{\sqrt{\varepsilon}}}+\left(0.16317+1.87\times10^{-12}\sqrt{\varepsilon}\right)e^{\frac{-1}{\sqrt{\varepsilon}}}-0.42630+0.10025,$$

$$k_{2}=\left(0.16317+1.87\times10^{-12}\sqrt{\varepsilon}\right)e^{\frac{-2}{\sqrt{\varepsilon}}}+0.16317-0.4263e^{\frac{-1}{\sqrt{\varepsilon}}}+0.100254e^{\frac{-3}{\sqrt{\varepsilon}}}-1.87\times10^{-12}\sqrt{\varepsilon},$$

$$k_{3}=\left(-0.16317+1.8669\times10^{-12}\sqrt{\varepsilon}\right)e^{\frac{-2}{\sqrt{\varepsilon}}}-0.16317-0.100254e^{\frac{-1}{\sqrt{\varepsilon}}}+0.4263e^{\frac{-3}{\sqrt{\varepsilon}}}-1.8669\times10^{-12}\sqrt{\varepsilon},$$

$$k_{4}=\left(-0.16317-1.8669\times10^{-12}\sqrt{\varepsilon}\right)e^{\frac{-3}{\sqrt{\varepsilon}}}+\left(-0.16317+1.8669\times10^{-12}\sqrt{\varepsilon}\right)e^{\frac{-1}{\sqrt{\varepsilon}}}-0.100254+0.4263e^{\frac{-2}{\sqrt{\varepsilon}}}.$$

Figure 7 illustrates the profile of the approximate second derivative solution for Example 3 at k=8, considering various values of ε. The distribution of the pointwise residual error over the entire problem domain and interior layer region is shown in Figure 8. Additionally, Figure 9 presents this error distribution over the left and right boundary regions. The results from Figures 7–9 show that decreasing ε improves solution accuracy. Moreover, the method produces accurate solutions not only over the outer regions but also within the boundary and interior layer regions.

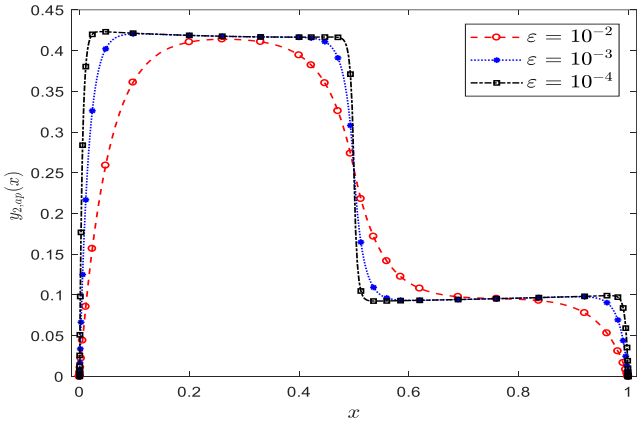

Figure 7. Approximate solution profile for the second derivative solution of Example 3 at $k = 8$ for various values of ε.

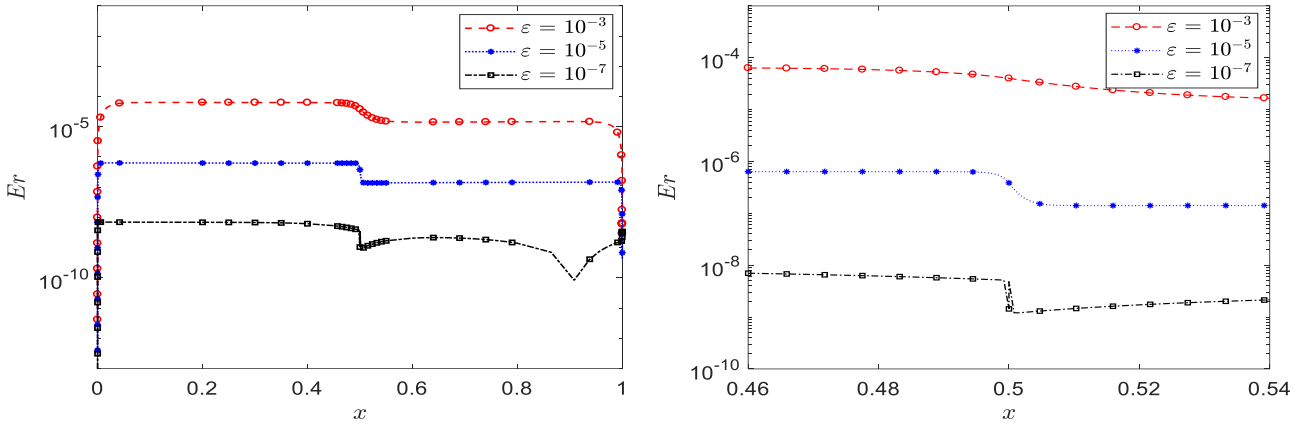

Figure 8. The pointwise residual error for the second derivative of Example 3 at $k = 8$ over (left) problem's domain and (right) the interior region, for various values of ε.

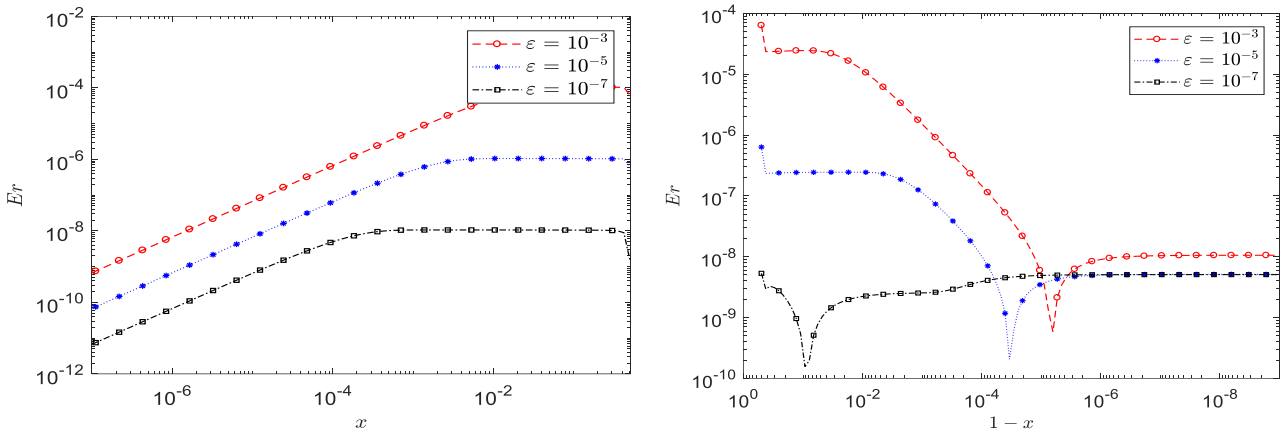

Figure 9. The pointwise residual error for the second derivative of Example 3 at $k = 8$ over (left) the left region and (right) the right region, for various values of ε.

Table 7 summarizes the maximum residual error, Er_{max}, and the CPU computational time required for solving Example 3 using the RPSM and RPSPM methods. It presents the results obtained for varying values of ε and k.In Tables 8–10, a comparison of the maximum pointwise error in the second derivative solution is presented. This comparison includes the results obtained using the present method and three other asymptotic numerical methods: the finite difference method [21], the finite element method [23], and the hybrid difference scheme [25]. Results in [23,25] are specifically presented for $\varepsilon = 10^{-16}$ and $\varepsilon = 2^{-1}-2^{-31}$, respectively, using different numbers of grid points. Notably, both studies achieved the highest accuracy when employing 1024 grid points. As a result, Tables 9 and 10 exclusively present these specific results to enable a meaningful comparison between the methods. The numerical results clearly demonstrate that the proposed method achieves higher accuracy compared to other numerical methods available in the literature, even when utilizing a smaller number of RPSPM terms.

Table 7. Maximum residual error ER_ε^N for Example 3 using RPSM and RPSPM at different values of ε.

ε	RPSM			RPSPM		
	$k=4$	$k=6$	$k=8$	$k=4$	$k=6$	$k=8$
10^{-1}	5.613741E-03	5.809664E-03	5.808063E-03	5.796096E-03	5.807787E-03	5.808052E-03
10^{-2}	2.620087E-04	6.351511E-04	6.362022E-04	8.773234E-04	6.366041E-04	6.362037E-04
10^{-3}	5.379639E-04	6.235163E-05	6.362440E-05	3.342862E-04	6.418149E-05	6.362690E-05
10^{-4}	5.970264E-04	5.065715E-06	6.360654E-06	2.799766E-04	6.933264E-06	6.363266E-06
10^{-5}	6.029327E-04	1.537519E-06	6.342798E-07	2.745456E-04	1.208441E-06	6.369024E-07
10^{-6}	6.035233E-04	2.110496E-06	6.164231E-08	2.740025E-04	6.359591E-07	6.426606E-08
10^{-7}	6.035824E-04	2.167794E-06	4.378570E-09	2.739482E-04	5.787109E-07	7.002425E-09
10^{-8}	6.035883E-04	2.173523E-06	2.813543E-09	2.739428E-04	5.729861E-07	1.276061E-09
10^{-9}	6.035889E-04	2.174096E-06	3.386180E-09	2.739422E-04	5.724136E-07	7.034249E-10
10^{-10}	6.035889E-04	2.174154E-06	3.443444E-09	2.739422E-04	5.723563E-07	6.461613E-10
10^{-20}	6.035889E-04	2.174160E-06	3.449807E-09	2.739422E-04	5.723500E-07	6.397986E-10
10^{-30}	6.035889E-04	2.174160E-06	3.449807E-09	2.739422E-04	5.723500E-07	6.397986E-10
CPU time (sec)	0.086	0.091	0.092	0.099	0.100	0.102

Table 8. Maximum pointwise error for Example 3 at different values of ε.

ε	Finite difference method [21] (1024 points)	Present method E_{max}^k			
		$k=4$	$k=6$	$k=8$	$k=10$
2^{-4}	4.64790E-05	1.399335E-06	1.777524E-08	4.934911E-12	9.135589E-14
2^{-6}	1.57036E-05	2.033085E-06	1.056671E-09	4.702997E-12	9.135589E-14
2^{-8}	1.47904E-05	2.350385E-06	7.313836E-09	4.586885E-12	9.135591E-14
2^{-10}	2.38508E-05	2.509035E-06	1.149909E-08	4.528828E-12	9.135591E-14
2^{-20}	6.94328E-05	2.662728E-06	1.555356E-08	4.472586E-12	9.135589E-14
2^{-21}	6.94319E-05	2.664180E-06	1.559186E-08	4.472055E-12	9.135589E-14

Table 9. Maximum pointwise error for Example 3 at $\varepsilon = 10^{-16}$.

Finite element method [23] (1024 points)		Present method E_{max}^k			
Shishkin mesh	*Bakhavlov-Shishkin mesh*	$k=4$	$k=6$	$k=8$	$k=10$
2.9542E-04	9.2591E-07	2.667686E-06	1.568435E-08	4.470772E-12	9.135590E-14

Table 10. Maximum pointwise error for Example 3 at $\varepsilon = 2^{-1}-2^{-31}$.

Hybrid difference scheme [25] (1024 points)	Present method E_{max}^k			
	$k=4$	$k=6$	$k=8$	$k=10$
9.1442E-3	5.214806E-07	6.844712E-08	5.637811E-12	9.135590E-14

Example 4. Consider the following fourth-order SPBVP with non-smooth variable coefficients (see [26,27]):

$$-\varepsilon y^{(iv)}(x) + b(x)y''(x) - y(x) = f(x), \quad x \in (\Omega^- \cup \Omega^+), \tag{37}$$

where

$$b(x) = \begin{cases} 2x+1\ , & 0 \le x \le 0.5, \\ 2(1-x)+1\ , & 0.5 < x \le 1, \end{cases}$$

$$f(x) = \begin{cases} 0.5\ , & 0 \le x \le 0.5, \\ -0.5\ , & 0.5 < x \le 1, \end{cases}$$

and

$$y(0) = y(1) = 1\ ,\ y''(0) = y''(1) = -0.5. \tag{38}$$

By employing the 8^{th}-order RPSPM, the piecewise approximate analytical solution is given by

$$y^8_{1,ap} = \begin{cases} \dfrac{1 + 2.4474x + 1.7264x^2 + 9.0743 \times 10^{-1}x^3 + 4.6349 \times 10^{-1}x^4}{1 + 2.8736x + 2.2009x^2 + 2.6116 \times 10^{-1}x^3 - 6.8567 \times 10^{-2}x^4} - \dfrac{\varepsilon}{2}\left(2k_1 e^{\frac{-1}{\sqrt{\varepsilon}}} + k_3 e^{\frac{2x-1}{\sqrt{2\varepsilon}}}\right), \\ 0 \le x \le 0.5, \\ \dfrac{3.7197 - 2.7197x + 1.9313^0(x-1)^2 - 3.0061 \times 10^{-1}(x-1)^3 + 5.0840 \times 10^{-2}(x-1)^4}{3.9553 - 2.9553x + 2.3775(x-1)^2 - 3.2788 \times 10^{-1}(x-1)^3 - 8.4472 \times 10^{-2}(x-1)^4} - \dfrac{\varepsilon}{2}\left(k_2 e^{\frac{1-2x}{\sqrt{2\varepsilon}}} + 2k_4 e^{\frac{x-1}{\sqrt{\varepsilon}}}\right), \\ 0.5 < x \le 1, \end{cases}$$

$$y^8_{2,ap} = \begin{cases} \dfrac{1.5 + 2.7117x + 1.2812x^2 + 5.7681 \times 10^{-1}x^3 + 1.4919 \times 10^{-1}x^4}{1 + 4.0919x + 5.1322x^2 + 1.8855x^3 - 2.6573 \times 10^{-2}x^4} - \left(k_1 e^{\frac{-1}{\sqrt{\varepsilon}}} + k_3 e^{\frac{2x-1}{\sqrt{2\varepsilon}}}\right), \\ 0 \le x \le 0.5, \\ \dfrac{1.3357 - 8.3572 \times 10^{-1}x + 2.6924 \times 10^{-1}(x-1)^2 - 9.8149 \times 10^{-2}(x-1)^3 + 3.8413 \times 10^{-2}(x-1)^4}{5.1426 \times 10^0 - 4.1426 \times 10^0 x + 5.3334(x-1)^2 - 2.1269(x-1)^3 + 5.7625 \times 10^{-2}(x-1)^4} - \left(k_2 e^{\frac{1-2x}{\sqrt{2\varepsilon}}} + k_4 e^{\frac{x-1}{\sqrt{\varepsilon}}}\right), \\ 0.5 < x \le 1, \end{cases}$$

where

$$k_1 = \left(35.3553 - 46.3922\sqrt{\varepsilon}\right)\mathrm{e}^{-\frac{0.707107}{\sqrt{\varepsilon}}} + \left(24.9999 + 46.3922\sqrt{\varepsilon}\right)\mathrm{e}^{-\frac{1.91421}{\sqrt{\varepsilon}}} + 162.132\mathrm{e}^{-\frac{1.20711}{\sqrt{\varepsilon}}} - 282.843,$$

$$k_2 = \left(-24.9999 + 46.3922\sqrt{\varepsilon}\right)\mathrm{e}^{-\frac{1.20711}{\sqrt{\varepsilon}}} - 46.3922\sqrt{\varepsilon} - 100\mathrm{e}^{-\frac{1.70711}{\sqrt{\varepsilon}}} - 35.3553 + 220.711\mathrm{e}^{-\frac{0.5}{\sqrt{\varepsilon}}},$$

$$k_3 = \left(24.9999 + 46.3922\sqrt{\varepsilon}\right)\mathrm{e}^{-\frac{1.20711}{\sqrt{\varepsilon}}} - 46.3922\sqrt{\varepsilon} - 200\mathrm{e}^{-\frac{1.70711}{\sqrt{\varepsilon}}} + 35.3553 + 79.2893\mathrm{e}^{-\frac{0.5}{\sqrt{\varepsilon}}},$$

$$k_4 = \left(-35.3553 - 46.3922\sqrt{\varepsilon}\right)\mathrm{e}^{-\frac{0.707107}{\sqrt{\varepsilon}}} + \left(-24.9999 + 46.3922\sqrt{\varepsilon}\right)\mathrm{e}^{-\frac{1.91421}{\sqrt{\varepsilon}}} + 262.132\mathrm{e}^{-\frac{1.20711}{\sqrt{\varepsilon}}} - 141.421.$$

Figure 10 depicts the profile of the approximate second derivative solution of Example 4 at $k = 8$ for different values of ε.

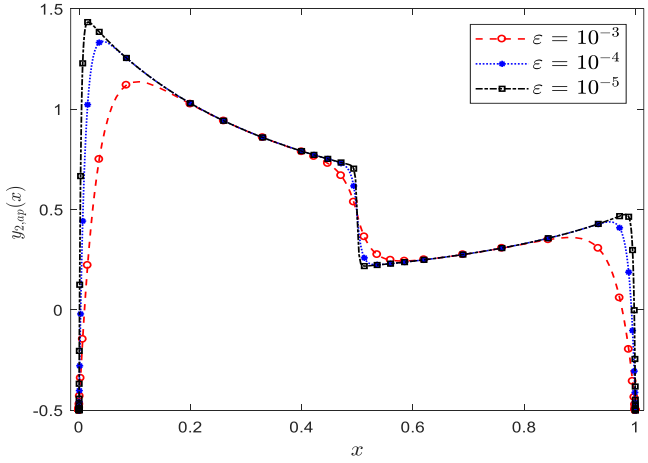

Figure 10. Approximate solution profile for the second derivative solution of Example 4 at $k = 8$, for various values of ε.

In Figure 11, the distribution of the pointwise residual error is shown over the entire problem's domain and the interior layer region. Furthermore, Figure 12 presents this error distribution over the left and right boundary regions. The results from Figures 11 and 12 validate that the method yields accurate solutions not only in the outer regions but also within the interior and boundary layer regions.

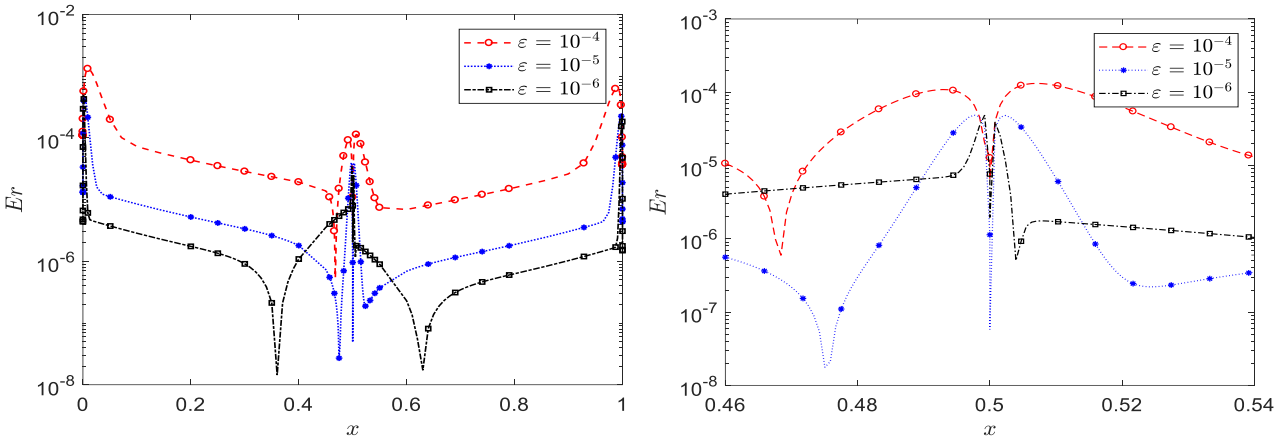

Figure 11. The pointwise residual error for the second derivative of Example 4 at $k = 8$ over (left) problem's domain and (right) the interior region, for various values of ε.

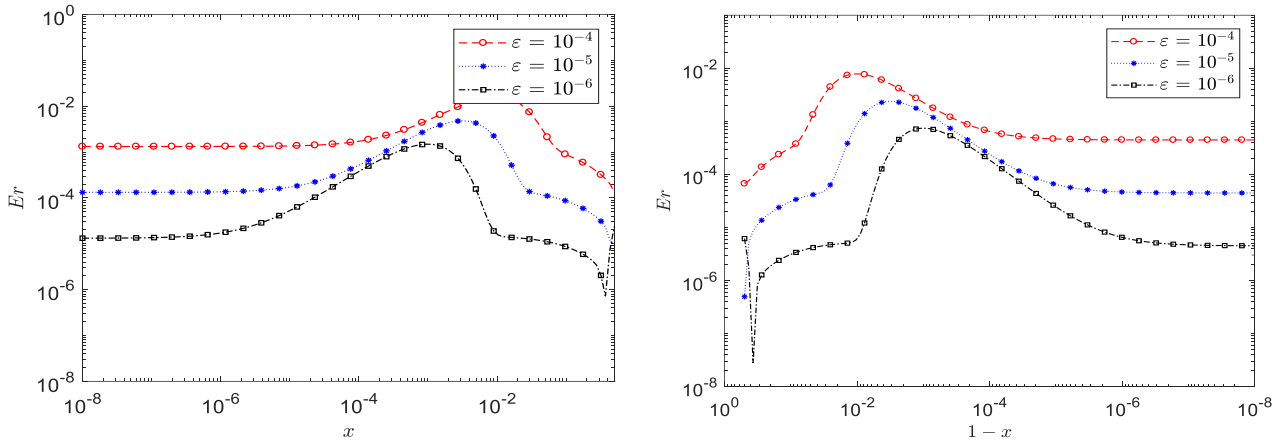

Figure 12. The pointwise residual error for the second derivative of Example 4 at $k = 8$ over (left) the left region and (right) the right region, for various values of ε.

Table 11 summarizes the maximum residual error, Er_{max}, and the CPU computational time required for solving Example 4 using the RPSM and RPSPM methods. It presents the results obtained for varying values of ε and k. Table 12 compares the maximum pointwise error in the second derivative solution between the present method and the asymptotic Schwarz method in [26]. The numerical results clearly demonstrate that the proposed method achieves higher accuracy compared to the results obtained in [26].

Table 11. Maximum residual error ER_ε^N for Example 4 using RPSM and RPSPM at different values of ε.

ε	RPSM			RPSPM		
	$k=4$	$k=6$	$k=8$	$k=4$	$k=6$	$k=8$
10^{-2}	1.385858E+00	5.718286E-01	5.980411E-01	1.318721E-01	1.318584E-01	1.318579E-01
10^{-3}	1.987772E+00	1.931463E+00	1.827591E+00	1.320589E-02	1.320451E-02	1.320446E-02
10^{-4}	2.046621E+00	2.066084E+00	2.068812E+00	9.340421E-03	1.320451E-03	1.320446E-03
10^{-5}	2.052505E+00	2.079546E+00	2.092934E+00	9.494831E-03	4.732560E-04	1.320446E-04
10^{-6}	2.053093E+00	2.080892E+00	2.095346E+00	9.510261E-03	4.876588E-04	2.398532E-05
10^{-7}	2.053152E+00	2.081027E+00	2.095587E+00	9.511803E-03	4.890987E-04	2.541258E-05
10^{-8}	2.053158E+00	2.081040E+00	2.095611E+00	9.511958E-03	4.892427E-04	2.555529E-05
10^{-9}	2.053159E+00	2.081042E+00	2.095614E+00	9.511973E-03	4.892571E-04	2.556956E-05
10^{-10}	2.053159E+00	2.081042E+00	2.095614E+00	9.511975E-03	4.892586E-04	2.557099E-05
10^{-20}	2.053159E+00	2.081042E+00	2.095614E+00	9.511975E-03	4.892587E-04	2.557115E-05
10^{-30}	2.053159E+00	2.081042E+00	2.095614E+00	9.511975E-03	4.892587E-04	2.557115E-05
CPU time (sec)	0.110	0.119	0.121	0.118	0.123	0.127

Table 12. Maximum pointwise error E_ε^k for Example 4 at different values of ε.

ε	Asymptotic Schwarz method [26]	Present method			
	(512 points)	$k=6$	$k=8$	$k=10$	$k=12$
2^{-4}	4.2220E-04	5.453675E-05	1.961521E-06	1.005865E-07	3.787474E-09
2^{-8}	1.2985E-05	8.979786E-05	3.200372E-06	1.291883E-07	4.373252E-09
2^{-12}	2.2938E-04	9.877568E-05	3.515795E-06	1.384381E-07	4.522396E-09
2^{-16}	5.5619E-04	1.010201E-04	3.594651E-06	1.407506E-07	4.559683E-09
2^{-20}	5.6036E-04	1.015813E-04	3.614365E-06	1.413287E-07	4.569004E-09
2^{-24}	5.6142E-04	1.017215E-04	3.619293E-06	1.414732E-07	4.571335E-09
2^{-50}	5.6142E-04	1.017215E-04	3.619293E-06	1.414732E-07	4.572111E-09

Results in Tables 1,5,7 and 11 show that, for RPSM/ RPSPM and for fixed k values, decreasing the perturbation parameter ε improves the solution accuracy. This improvement in accuracy can be attributed to the reduction of the asymptotic error until the RPSM/ RPSPM error becomes more prominent. Moreover, as the RPSM/ RPSPM error dominates, increasing the order k further enhances the accuracy. It is worth noting that RPSPM demonstrates a significantly greater enhancement in accuracy compared to RPSM, particularly for SPBVPs with variable coefficients as shown in Examples 2 and 4. Furthermore, RPSPM overcomes the challenge of approximating the solution of SPBVPs with discontinuous coefficients, unlike RPSM which fails in this regard as shown in the Example 4. These results suggest that decreasing the perturbation parameter and increasing the order of the RPSPM method improve the accuracy of the solution, aligning with the theoretical results obtained in this study.

Results in Tables 1,5,7 and 11 show that the method's efficiency and the low computational cost are evident from the CPU time values. Furthermore, varying the perturbation parameter, ε, does not affect the computational time due to the independence of the reduced problems' solutions. Additionally, increasing the method's order, k, slightly increases the computational time because only two new terms are required to be added to the RPSM and Padé approximations, which are readily obtained using built-in Maple functions, making the computational overhead minimal.

Although the suggested method is primarily designed for third- and fourth-order reaction-

diffusion SPBVPs with a discontinuous source term, it can be extended to a wider range of problems. Specifically, the method has been shown to be applicable to problems with non-smooth variable coefficients (as demonstrated in Example 4). Furthermore, the method can be extended to convection-diffusion SPBVPs using appropriate asymptotic approximations [12,13,24]. Similarly, it can be extended to nonlinear problems using the linearization techniques [41] for reaction-diffusion problems and an appropriate asymptotic approximation for quasilinear convection-diffusion problems.

6. Conclusions

This paper introduces a reliable algorithm for developing piecewise approximate analytical solutions to high-order reaction-diffusion SPBVPs with a discontinuous source term. These problems have practical applications, and an approximate analytical solution is needed to gain insights into their behavior and analyze practical scenarios considering different physical parameters. The algorithm transforms the problem into a weakly coupled system of ordinary differential equations. A zero-order asymptotic approximate solution is then provided, resulting in known solutions for the boundary and interior layers. The outer region solution is obtained analytically using the RPSPM, which incorporates Padé approximant, renowned for their higher accuracy and fast convergence compared to RPSM series approximation. By applying the RPSPM, a piecewise smooth solution for the reduced problem is obtained, satisfying continuity and smoothness conditions. Consequently, a piecewise approximate analytical solution for the original SPBVP is obtained. Thus, the method provides approximate analytical solutions while most other methods in the literature are numerical in nature. The algorithm is successfully validated on various third and fourth-order SPBVPs with constant and variable coefficients. The numerical results highlight the advantages of reducing the perturbation parameter, ε, and increasing the order, k, for enhancing the solution accuracy, which is consistent with theoretical results. Results in figures confirm that the present method can yield accurate solutions in all regions, including interior and boundary layers. Moreover, the present numerical comparisons confirm that the present RPSPM is more accurate than the standard RPSM and other numerical asymptotic methods like finite difference [22], finite element [23], hybrid difference scheme [25], and Schwarz method [26] in solving the considered problems. The computational efficiency of the method is evidenced by the low CPU time values. Furthermore, the CPU time is insensitive to variations in the perturbation parameter, ε, due to the independence of the reduced problems' solutions. Minimal computational overhead occurs when increasing the method's order, k, as only a few new series terms need to be added to the RPSM and Padé approximations. The method can be extended to a wider range of problems, including those with non-smooth variable coefficients, as demonstrated in Example 4. Overall, the proposed algorithm offers a convenient and reliable approach for effectively addressing high-order reaction-diffusion SPBVPs with a discontinuous source term in a new asymptotic semi-analytical numerical framework. Our future research will focus on extending the method's capabilities to encompass nonlinear problems, a wider variety of higher-order SPBVPs with non-smooth variable coefficients and discontinuous source terms, and more applications with physical interpretation of the parameters and solution behavior.

Use of AI tools declaration

The authors declare they have not used Artificial Intelligence (AI) tools in the creation of this article.

Acknowledgments

We gratefully acknowledge the reviewers for their thorough evaluation and valuable feedback, which significantly improved the quality of our paper. This study is supported via funding from Prince Sattam bin Abdulaziz University (project number PSAU/2024/R/1445).

Conflict of interest

The authors declare no conflicts of interest.

References

1. P. V. Kokotović, Applications of singular perturbation techniques to control problems, *SIAM Rev.*, **26** (1984), 501–550. https://doi.org/10.1137/1026104
2. A. J. Chamkha, A. M. Rashad, E. R. El-Zahar, H. A. EL-Mky, Analytical and numerical investigation of Fe_3O_4-water nanofluid flow over a moveable plane in a parallel stream with high suction, *Energies*, **12** (2019), 198. https://doi.org/10.3390/en12010198
3. P. W. Hsieh, Y. Shih, S. Y. Yang, A tailored finite point method for solving steady MHD duct flow problems with boundary layers, *Commun. Comput. Phys.*, **10** (2011), 161–182. https://doi.org/10.4208/cicp.070110.020710a
4. M. Amir, Q. Ali, A. Raza, M. Y. Almusawa, W. Hamali, A. H. Ali, Computational results of convective heat transfer for fractionalized Brinkman type tri-hybrid nanofluid with ramped temperature and non-local kernel, *Ain Shams Eng. J.*, **15** (2024), 102576. https://doi.org/10.1016/j.asej.2023.102576
5. O. Nave, M. Sharma, Singular perturbed vector field (SPVF) applied to complex ode system with hidden hierarchy application to turbocharger engine model, *Int. J. Nonlinear Sci. Numer. Simul.*, **21** (2019), 99–113. https://doi.org/10.1515/ijnsns-2019-0024
6. G. P. Thomas, Towards an improved turbulence model for wave-current interactions, *2nd Annual Report to EU MAST-III Project The Kinematics and Dynamics of Wave-Current Interactions*,1988.
7. R. O'Malley, *Introduction to singular perturbations*, Academic Press, 1974.
8. J. Kevorkian, J. D. Cole, *Perturbation methods in applied mathematics*, Springer Science & Business Media, 1981. https://doi.org/10.1007/978-1-4757-4213-8
9. J. J. Miller, E. O'Riordan, G. Shishkin, *Fitted numerical methods for singular perturbation problems*, World Scientific, 2012.
10. C. S. Liu, E. R. El-Zahar, C. W. Chang, Higher-order asymptotic numerical solutions for singularly perturbed problems with variable coefficients, *Mathematics*, **10** (2022), 2791. https://doi.org/10.3390/math10152791
11. E. R. El-Zahar, S. M. El-Kabeir, A new method for solving singularly perturbed boundary value problems, *Appl. Math. Inf. Sci.*, **7** (2013), 927. https://doi.org/10.12785/amis/070329
12. E. R. El-Zahar, Approximate analytical solutions of singularly perturbed fourth order boundary value problems using differential transform method, *J. King Saud Univ.*, **25** (2013), 257–265. https://doi.org/10.1016/j.jksus.2013.01.004
13. E. R. El-Zahar, Piecewise approximate analytical solutions of high-order singular perturbation problems with a discontinuous source term, *Int. J. Differ. Equations*, **2016** (2016), 1015634. https://doi.org/10.1155/2016/1015634

14. T. Valanarasu, N. Ramanujam, Asymptotic initial-value method for a system of singularly perturbed second-order ordinary differential equations of convection-diffusion type, *Int. J. Comput. Math.*, **81** (2004), 1381–1393. https://doi.org/10.1080/0020716042000293187
15. W. G. Melesse, A. A. Tiruneh, G. A. Derese, Solving systems of singularly perturbed convection diffusion problems via initial value method, *J. Appl. Math.*, **2020** (2020), 1062025. https://doi.org/10.1155/2020/1062025
16. S. Valarmathi, N. Ramanujam, An asymptotic numerical method for singularly perturbed third-order ordinary differential equations of convection-diffusion type, *Comput. Math. Appl.*, **44** (2002), 693–710. https://doi.org/10.1016/S0898-1221(02)00183-9
17. J. C. Roja, A. Tamilselvan, Numerical method for singularly perturbed third order ordinary differential equations of convection-diffusion type, *Numer. Math.*, **7** (2014), 265–287. https://doi.org/10.1017/S1004897900000118
18. M. Cui, F. Geng, A computational method for solving third order singularly perturbed boundary-value problems, *Appl. Math. Comput.*, **198** (2008), 896–903. https://doi.org/10.1016/j.amc.2007.09.023
19. V. Shanthi, N. Ramanujam, A boundary value technique for boundary value problems for singularly perturbed fourth-order ordinary differential equations, *Comput. Math. Appl.*, **47** (2004), 1673–1688. https://doi.org/10.1016/j.camwa.2004.06.015
20. M. I. Syam, B. S. Attili, Numerical solution of singularly perturbed fifth order two-point boundary value problem, *Appl. Math. Comput.*, **170** (2005), 1085–1094. https://doi.org/10.1016/j.amc.2005.01.003
21. V. Shanthi, N. Ramanujam, An asymptotic numerical method for fourth order singular perturbation problems with a discontinuous source term, *Int. J. Comput. Math.*, **85** (2008), 1147–1159. https://doi.org/10.1080/00207160701478862
22. T. Valanarasu, N. Ramanujam, Asymptotic numerical method for singularly perturbed third order ordinary differential equations with a discontinuous source term, *Novi Sad J. Math.*, **37** (2007), 41–57.
23. A. R. Babu, N. Ramanujam, An asymptotic finite element method for singularly perturbed third and fourth order ordinary differential equations with discontinuous source term, *Appl. Math. Comput.*, **191** (2007), 372–380. https://doi.org/10.1016/j.amc.2007.02.093
24. A. R. Babu, N. Ramanujam, An asymptotic finite element method for singularly perturbed higher order ordinary differential equations of convection-diffusion type with discontinuous source term, *J. Appl. Math. Inf.*, **26** (2008), 1057–1069.
25. V. Shanthi, N. Ramanujam, An asymptotic hybrid difference scheme for singularly perturbed third and fourth order ordinary differential equations with discontinuous source term, *Neural Parallel Sci. Comput.*, **16** (2008), 327–336. https://doi.org/10.5555/1561709.1561712
26. M. Chandr, V. Shanthi, A Schwarz method for fourth-order singularly perturbed reaction-diffusion problem with discontinuous source term, *J. Appl. Math. Inf.*, **34** (2016), 495–508. http://doi.org/10.14317/jami.2016.495
27. P. C. Podila, V. Sundrani, H. Ramos, Numerical solution of a fourth-order singularly perturbed boundary value problem with discontinuities via Haar wavelets, *Math. Methods Appl. Sci.*, **45** (2022), 10904–10916. https://doi.org/10.1002/mma.8424
28. M. S. Alam, N. Sharif, M. H. U. Molla, Combination of modified Lindstedt-Poincare and homotopy perturbation methods, *J. Low Freq. Noise Vibration Active Control*, **42** (2022), 642–653. https://doi.org/10.1177/14613484221148049

29. N. H. Aljahdaly, A. M. Alweldi, On the modified Laplace homotopy perturbation method for solving damped modified Kawahara equation and its application in a fluid, *Symmetry*, **15** (2023), 394. https://doi.org/10.3390/sym15020394
30. S. R. M. Noori, N. Taghizadeh, Modified differential transform method for solving linear and nonlinear pantograph type of differential and Volterra integro-differential equations with proportional delays, *Adv. Differ. Equations*, **2020** (2020), 649. https://doi.org/10.1186/s13662-020-03107-9
31. B. Benhammouda, H. Vazquez-Leal, L. Hernandez-Martinez, Modified differential transform method for solving the model of pollution for a system of lakes, *Discrete Dyn. Nat. Soc.*, **2014** (2014), 645726. https://doi.org/10.1155/2014/645726
32. A. E. Ebaid, A reliable aftertreatment for improving the differential transformation method and its application to nonlinear oscillators with fractional nonlinearities, *Commun. Nonlinear Sci. Numer. Simul.*, **16** (2011), 528–536. https://doi.org/10.1016/j.cnsns.2010.03.012
33. S. Momani, O. A. Arqub, M. A. Hammad, Z. A. Hammour, A residual power series technique for solving systems of initial value problems, *Appl. Math. Inf. Sci.*, **10** (2016), 765–775. https://doi.org/10.18576/AMIS/100237
34. E. R. El-Zahar, G. F. Al-Boqami, H. S. Al-Juaydi, Approximate analytical solutions for strongly coupled systems of singularly perturbed convection-diffusion problems, *Mathematics*, **12** (2024), 277. https://doi.org/10.3390/math12020277
35. A. Dawar, H. Khan, S. Islam, W. Khan, The improved residual power series method for a system of differential equations: a new semi-numerical method, *Int. J. Model. Simul.*, **43** (2023), 1–14. https://doi.org/10.1080/02286203.2023.2270884
36. F. Chen, Q. Q. Liu, Adomian decomposition method combined with Padé approximation and Laplace transform for solving a model of HIV infection of $CD4^{+}T$ cells, *Discrete Dyn. Nat. Soc.*, **2015** (2015), 584787. https://doi.org/10.1155/2015/584787
37. W. B. Jones, W. J. Thron, On convergence of Padé approximants, *SIAM J. Math. Anal.*, **6** (1975), 9–16. https://doi.org/10.1137/0506002
38. J. Anderson, *Fundamentals of aerodynamics*, McGraw-Hill Education. https://doi.org/10.2514/152157
39. K. Stephan, *Heat transfer in condensation and boiling*, Springer-Verlag, 1992. https://doi.org/10.1007/978-3-642-52457-8
40. J. Jackson, *Classical electrodynamics*, Wiley, 1998.
41. R. Burden, J. D. Faires, A. M. Burden, *Numerical analysis*, Cengage Learning, 2021.